VIII. Cosmic Microwave background radiation

8.1. Measurements of the CMB

Predictions and Discovery

As we have discused in previous lectures there are more photons than any other type of baryonic matter in the Universe. The baryon to phonton ratio is:

$$\eta = \frac{n_b}{n_\gamma} = 10^{-10}\eta_{10} = 10^{10} \times 274\,\Omega_b\, h^2$$

This ratio was frozen in at BBN.

Considering radiation as a barygotropic fluid $(p = \omega \rho c^2)$ with $\omega = 1/3$, we find that the temperature of photons scales as $T \propto R^{-1}$

Even if their temperature dropped, we should be able to observe those photons today.

Let us start with a distribution of photons in thermal equilibrium. Their spectral energy distribution is given by the Planck curve:

$$u(\nu)\,d\nu = \frac{8\pi h\nu^3}{c^3}\frac{1}{e^{h\nu/k_BT}-1}\,d\nu$$

Since we know how ρ_{rad} scales with expansion on an adiabatically expanding Universe:

$T \propto R^{-1}$

$\rho \propto R^{-4} \iff \nu \propto R^{-1}$

We can introduce the expression of the energy distribution to obtain:

$$u(\tilde{\nu})\,d\tilde{\nu} = R^{-4}\frac{8\pi h\tilde{\nu}^3}{c^3}\frac{1}{e^{h\tilde{\nu}/k_B\tilde{T}}-1}\,d\tilde{\nu}$$

NOTE: $\rho_{rad} \propto R^{-4}$, as seen in the Thermal history lecture

Which is also a Planck curve with $\tilde{T} = T/R$.

Black-body radiation in an expanding Universe cools down, but remains thermal. (Tolman, 1934)

We should be able to detect those photons, but we need to know their temperature (and so, $R(t)$).

Historic predictions

1946. George Gamov predicts $T \approx 50k$

1948. Ralph Alpher and Robert Herman predict $T \approx 5k$

1960. Robert Dicke re-estimates $T \approx 40\,K$

1964. A Doroshkevich and Igor Novikov suggest to search for the CMB

Discovery

The discovery of the CMB was attributed to Penzias and Wilson (1965), but it was actually detected in 1957 by Emile Le Roux. This PhD student at Nancay Radio Observatory (France) found a near isotropic background of 3K at $\lambda = 33$ cm while he was doing a galaxy survey. However, this was removed from his article following a suggestion of her supervisor.

The CMB emission was (re)-discovered by Penzias & Wilson, who won the Nobel Prize in 1978. The detection and the possible explanation were published together on the same journal. The interpretation of the measurements was given by Dicke, Peebles & Wilkinson, following the work of Alpher, Bethe and Gamow.

Measurements of the CMB

Monopole

Once it was discovered, it was necessary to proof that this radiation corresponded to the one of a Black Body. This required to measure the photons emitted on the last scattering at various frequencies.

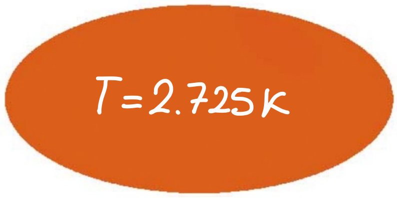

COBE satellite was launched in 1992 to the energy distribution of these background photons in every direction. The obtained data fitted very accurately to a blackbody with $\boxed{T = 2.725\,K}$ (better than the ones "created" in a laboratory).

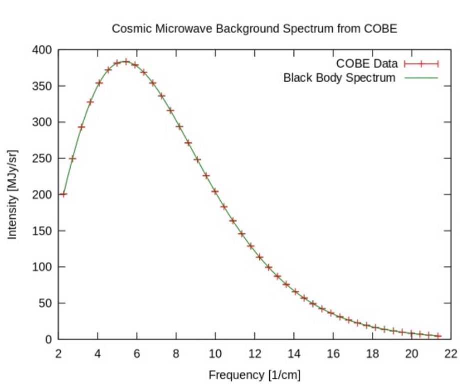

It was found that the distribution agreed with that temperature, but not for local patches: there were higher order terms. However, any deviation from $T = 2.725\,K$ was very small (even for the dipole).

Dipole

Looking into a 180° separation, we measure a marginally different temperature: $\boxed{\Delta T = 3.353\ mK}$

ΔT

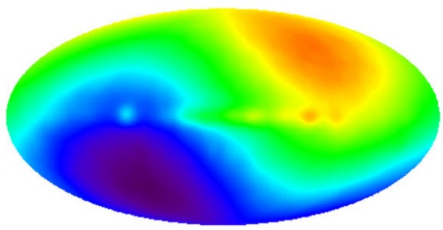

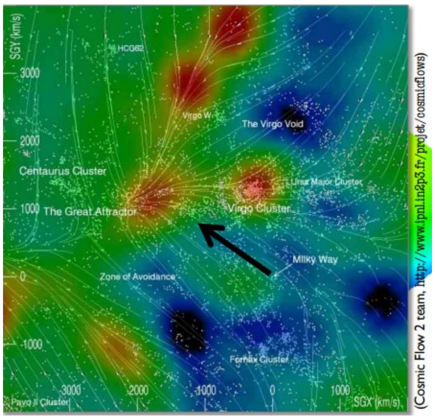

This difference in temperature indicates the existence of a dipole. It is caused by the movement of the Local Group towards the Great Attractor at ca. 627 km/s (Doppler shift). Measuring the dipole allows to infer the velocity of this movement. A dipole has to exist unless MW is at rest with respect to the CMB (otherwise we would be in a special coordinate frame, and that violates isotropy)

$\longrightarrow$ The dipole can only be explained by movement of the observer

Higher order anisotropies

There are also lots of higher order anisotropies (quadropoles, ...). There have been several missions to quantify them with the highest degree of accuracy as possible. The band in the middle is due to the Milky Way disc, which makes us unable to measure the anisotropies in that directions.

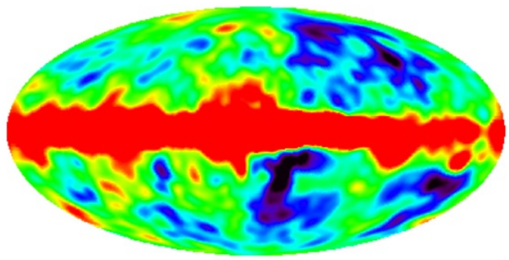

$\boxed{\Delta T = 18 \mu k}$

Some of the missions that aimed to measure the CMB anisotropies were:

1983: Launch of Russian satellite RELIKT-I (announced discovery of $\Delta T/T$ in 1992, but was unnoticed due to Cold War & lack of translation).

1990: launch of COBE satellite (Nobel Prize in 2006 for discovery of $\Delta T/T$).

1999: BOOMERanG and Maxima balloon experiments

2001: launch of WMAP satellite

2002: DASI discovers polarisation

2009: Launch of Planck satellite

After correcting the effect of the galactic disc, we can compare the accuracy of the different missions.

COBE satellite (1992)

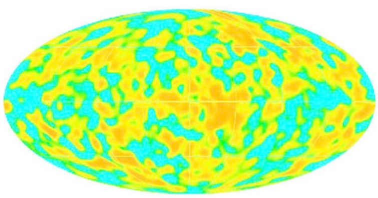

WMAP (2001)

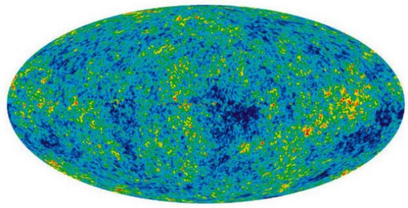

Planck (2015)

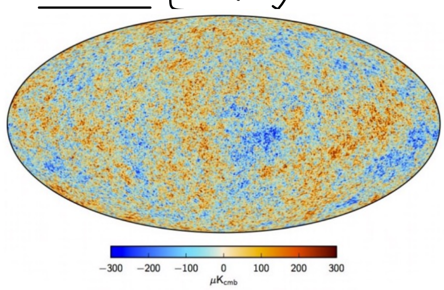

28:00

Our current values for H and the density parameters Ω (as well as other parameters) come from the data of the Planck satellite. It will be difficult to obtain better results than the ones from Planck satellite for Primary anisotropies.

8.2. Origin of the CMB anisotropies

Qualitative approach:

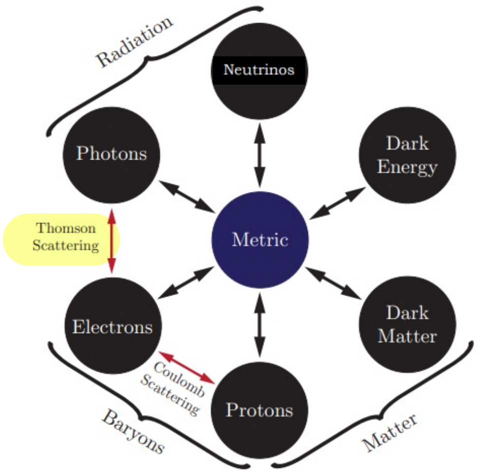

The interactions between different components establish couplings between them. Perturbations in one component reflect on the others (via direct interactions) as long as they are coupled. Even if all components are coupled by the metric, this is weaker than the direct interactions (however, it is important to remember that this coupling exists).

We only can have a coupling between radiation and baryons if there are free electrons (for Thomson scattering). Even after e^+e^- annihilation there are free electrons left, which are still coupled to the radiation.

- PRIOR TO RECOMBINATION

Electrons and photons are coupled by Thomson scattering. The Universe is opaque for radiation. There are also protons, which are combining with the electrons to form hydrogen. Once the electrons are captured, they are not available for scattering anymore. The union between electrons and protons is called RECOMBINATION.

BEFORE RECOMBINATION:

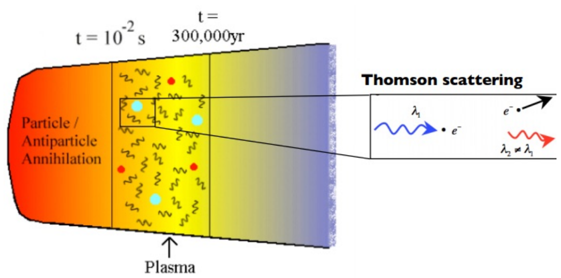

AFTER RECOMBINATION:

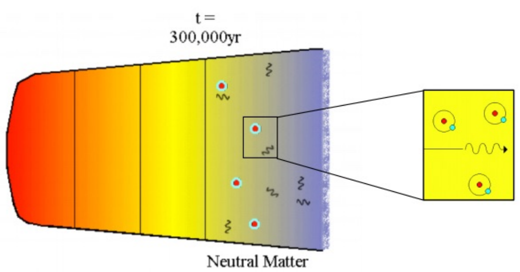

AFTER RECOMBINATION

Electrons are bound to protons and photons are free to travel. These are the CMB photons.

It is important to note that recombination and decoupling happened at different times: there is a short period in between.

We can calculate the times (temperatures) of both events to analyse what happened to photons and electrons.

CMBR origin calculation

Hydrogen recombination. Saha equation.

For recombination, we have the following reaction:

$$e^- + p \leftrightarrow H + \gamma \qquad \text{(in equilibrium)}$$

The number densities of the elements involved are:

$$n_e = g_e \left(\frac{m_e kT}{2\pi\hbar^2}\right)^{3/2} e^{-(m_e - \mu_e)c^2/kT} \qquad n_p = g_p \left(\frac{m_p kT}{2\pi\hbar^2}\right)^{3/2} e^{-(m_p - \mu_p)c^2/kT}$$

$$n_H = g_H \left(\frac{m_H kT}{2\pi\hbar^2}\right)^{3/2} e^{-(m_H - \mu_H)c^2/kT}$$

Since we are interested in a ratio, we calculate:

$$\left(\frac{n_H}{n_e n_p}\right) = \frac{g_H}{g_e g_p}\left(\frac{m_H}{m_e m_p}\frac{2\pi\hbar}{kT}\right)^{3/2} e^{(m_e + m_p - m_H)c^2/kT}$$

Binding energy of hydrogen

Where we have considered that, in equilibrium: $\mu_e + \mu_p = \mu_H \qquad \mu_\gamma = 0$

$$\left(\frac{n_H}{n_e n_p}\right) = \frac{g_H}{g_e g_p}\left(\frac{m_H}{m_e m_p}\frac{2\pi\hbar}{kT}\right)^{3/2} e^{B_H/kT}$$

Prefactors are known or assumed:

$n_e = n_p$ (charge neutrality) $\qquad g_e = g_p = 2$ (spin up-down)

$m_H \approx m_p$ (only for pre-factor) $\qquad g_H = 4$ (e aligned / antialigned to p)

Since the electrons are the ones coupled to photons, we express everything in terms of their number density (taking into account that $n_e \approx n_p$). Assuming that m_H is dominated by the proton mass:

$$\boxed{\left(\frac{n_H}{n_e^2}\right) = \left(\frac{2\pi\hbar}{m_e kT}\right)^{3/2} e^{B_H/kT}}$$

We are interested in the fraction of free electrons:

$$X_e = \frac{n_e}{n_b}$$

The density of baryons n_b can be written in terms of the density of photons as:

$n_b = \eta\, n_\gamma$, where:

$$n_\gamma = \frac{2\zeta(3)}{\pi^2}\left(\frac{k}{\hbar c}\right)^3 T^3 \qquad \eta \equiv \text{photon to baryon fraction}$$

Thus:

$$n_b = \eta\, n_\gamma = \eta\,\frac{2\zeta(3)}{\pi^2}\left(\frac{k}{\hbar c}\right)^3 T^3$$

We also know that the number density of baryons is given by (ignoring all nuclei A>1 and assuming charge neutrality):

$n_b \approx n_p + n_H = n_e + n_H$

We can rewrite the expresion obtained for n_H / n_e^2 as:

$$n_H = n_e^2 \left(\frac{2\pi\hbar}{m_e kT}\right)^{3/2} e^{B_H/kT}$$

And so:

$$n_b = n_e + n_H = n_e \left(1 + n_e \left(\frac{2\pi\hbar}{m_e kT}\right)^{3/2} e^{B_H/kT}\right)$$

We can rewrite the free-electron fraction as:

$$X_e = \frac{n_e}{n_b} \longrightarrow 1 = \frac{X_e n_b}{n_e}$$

And joining everything together:

$$1 = X_e\left(1 + n_e \left(\frac{2\pi\hbar}{m_e kT}\right)^{3/2} e^{B_H/kT}\right) \longrightarrow \frac{1}{X_e} = 1 + n_e \left(\frac{2\pi\hbar}{m_e kT}\right)^{3/2} e^{B_H/kT} \longrightarrow$$

$$\frac{1}{X_e} - 1 = n_e \left(\frac{2\pi\hbar}{m_e kT}\right)^{3/2} e^{B_H/kT} \longrightarrow \frac{1-X_e}{X_e} = n_e \left(\frac{2\pi\hbar}{m_e kT}\right)^{3/2} e^{B_H/kT} = X_e n_b \left(\frac{2\pi\hbar}{m_e kT}\right)^{3/2} e^{B_H/kT} \longrightarrow$$

$$\frac{1-X_e}{X_e^2} = \eta \frac{2\zeta(3)}{\pi^2}\left(\frac{k^2}{\hbar c}\right)^3 T^3 \left(\frac{2\pi\hbar^2}{m_e kT}\right)^{3/2} e^{B_H/kT} \longrightarrow \boxed{\frac{1-X_e}{X_e^2} = \frac{2\zeta(3)}{\pi^2}\eta\left(\frac{2\pi kT}{\hbar c^2 m_e}\right)^{3/2} e^{B_H/kT}}$$

Saha equation

This is a non-linear equation, so we cannot get an explicit formula $X_e = \ldots$ We have an intrinsic definition that can be solved numerically.

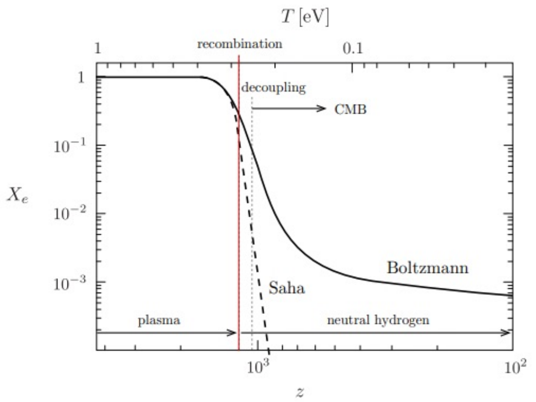

Solving the equation, we find that in the very early Universe, at temperatures ~1eV, all the electrons are free. When T drops, X_e drops too. The dashed line represents the result of Saha equation if no cosmology would happen in between.

We define the beginning of recombination as the point when we have $X_e = 0.1$ (i.e. the point where we only have 10% of the initial free electrons). This gives:

$\boxed{T = 0.31 \text{ eV}} \ll B_H$!

Naively, we could think that this temperature is too low because the binding energy of hydrogen is $B_H = 13.6$ eV: as soon as the temperature of the Universe (and so, the photons) is below 13.6 eV, the reaction should only go in the direction $e^- + p \rightarrow H + \gamma$ (photons do not have enough energy to dissociate H). However, we have to take into account that the number of photons is (way) larger than the number of baryons, so there are still photons with enough energy to dissociate H: η delays recombination. Translating this to redshift, recombination takes place around $\boxed{z_{rec} = 1300}$

In another lecture we calculated the redshift for matter-radiation equality ($z_{eq} \approx 3400$, using Planck cosmology). Thus, recombination happens during matter domination.

Photon decoupling

After recombination, we still have some free electrons (10% of the initial quantity). Those electrons still interact with the photons. This stops at decoupling. We can calculate when does it happen through the interaction rate of Thomson scattering:

$e^- + \gamma \leftrightarrow e^- + \gamma$

Electrons will decouple when $\Gamma / H < 0.1$:

$$\Gamma_\gamma \approx n_e \sigma_T c = n_b X_e \sigma_T c = \eta \frac{2\zeta(3)}{\pi^2} \left(\frac{k}{\hbar c}\right)^3 T^3 X_e \sigma_T c$$

$H = (H_0^2 \Omega_{m,0} R^{-3})^{1/2}$ matter domination (as $z_{rec} << z_{eq}$), from Friedmann equation

And taking into account the scaling with temperature: $T \propto R^{-1}$

$H = H_0 \sqrt{\Omega_{m,0}} \left(\frac{T}{T_0}\right)^{3/2}$ where T is the temperature of the photons

Equating both expressions, we use Saha equation for X_e (T_{dec}) and solve for T_{dec}.

$$\eta \frac{2\zeta(3)}{\pi^2} \left(\frac{k}{\hbar c}\right)^3 T_{dec}^3 X_e \sigma_T c \approx H_0 \sqrt{\Omega_{m,0}} \left(\frac{T_{dec}}{T_0}\right)^{3/2}$$

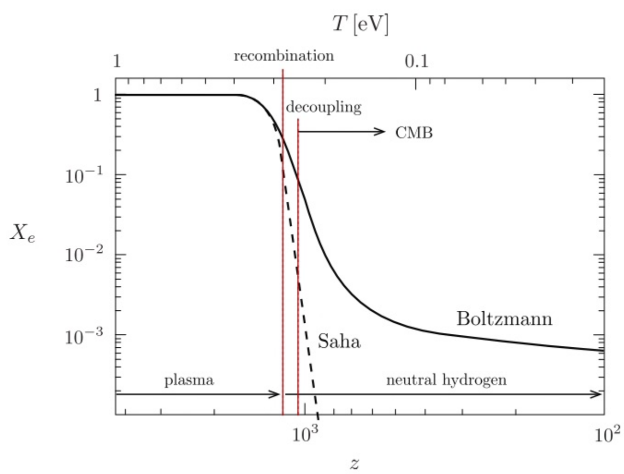

Numerically, we find that:

$$\boxed{\begin{aligned} T_{dec} &= 0.27 \text{ eV} \\ z_{dec} &= 1090 \end{aligned}}$$

Both recombination and decoupling happen at approximately the same temperature, but decouple happens a bit later.

A proper (more accurate) calculation would require solving the Boltzmann equation.

$z = 1090$ (decoupling) defines the last scattering surface. From that onwards we are able to see the Universe.

8.3. CMB fluctuations

Primary fluctuations

Intrinsic fluctuations

Before the emision of the CMB, everything was homogeneous and isotropic. Afterwards, during the evolution of the Universe, non-linearities are developing, giving rise to non-isotropic and non homogeneous structures. There must be some primordial matter fluctuations acting as seeds for all the structures in the Universe.

At inflation, quantum fluctuations grew up and became macroscopic (but they were still tiny): primordial matter fluctuations. These structures grew gravitationally over time, and lead to intrinsic fluctuations in the CMB (which are conserved).

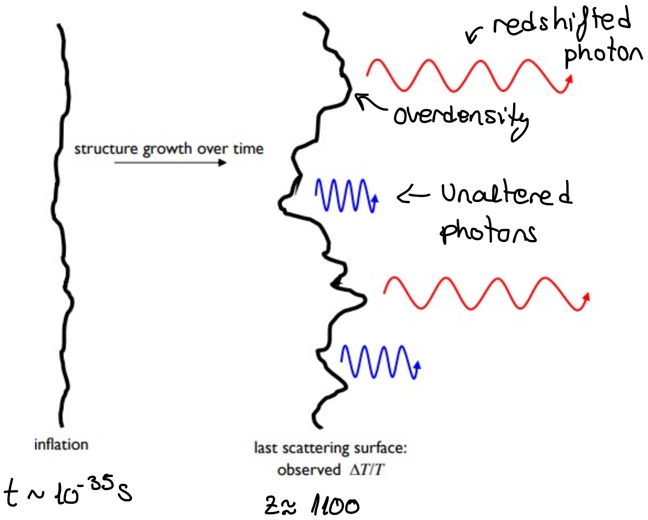

At the time of electron decoupling, photons are free to travel. A photon that starts travelling from an overdense region will be gravitationally redshifted (because it must scape from the potential well). Redshifted photons will have a lower temperature than unaltered photons since $E = h\nu = KT$

Cold spots in CMB $\equiv$ high density regions
Hot spots in CMB $\equiv$ low density regions

Matter structures keep growing over time. Today, we observe $\Delta\rho_m/\rho_m$ and $\Delta T/T$. The latter are the reflection of the anisotropies in the matter distribution at $z \sim 1100$.

We can make predictions about $\Delta T/T$ at that redshift based on the $\Delta\rho_m/\rho_m$ that we observe today.

Since the photons are decoupled, they evolve as $T_\gamma \propto R^{-1}$. Therefore, $\Delta T/T$ is not changing:

$T \propto R^{-1}$, $\boxed{\Delta T/T = \text{const}}$

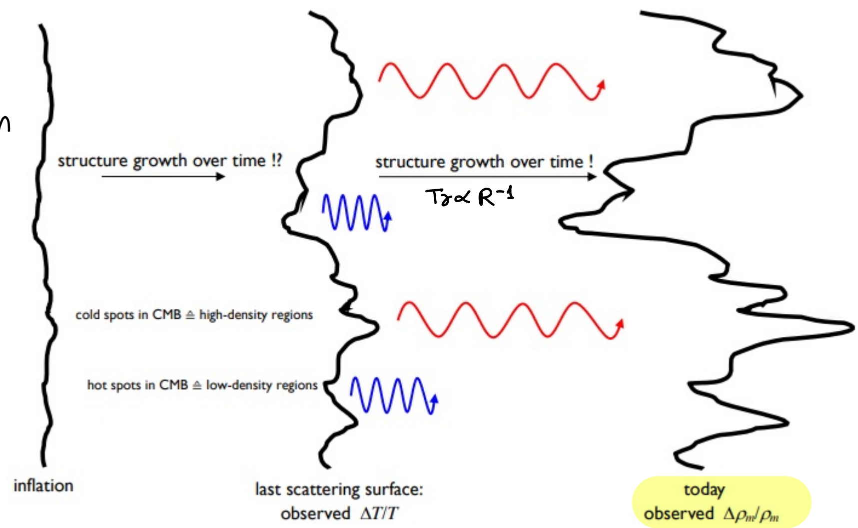

We want to obtain $\Delta T/T$ and a relation such as $\Delta T/T = K \, \Delta\rho_m/\rho_m$

The first step will be translating the $\Delta\rho_m/\rho_m$ that we observe today back to its value at decoupling. To do so, we can use the following equation for the evolution of the density contrast:

$$\boxed{\ddot{\delta}_m + 2H\dot{\delta}_m = 4\pi G\rho_m \delta_m} \qquad \delta_m = \frac{\Delta\rho}{\rho}$$

For a matter dominated Universe with $\Omega_m = 1$, we get:

$$\delta_{m,0} = \delta_{m,dec}\, a$$

Today, we observe that $\delta_{m,0} \gtrsim 1$. This is a lower limit, since taking two galaxies and the background gives a higher value ($\sim 10^6$)

We know the value of redshift for decoupling ($z \approx 1100$), so we can scale δ $\left(a = \frac{1}{1+z}\right)$ and find:

$$\boxed{\delta_{m,dec} \gtrsim 10^{-3}}$$ which is, again, a lower limit.

Now we need to relate it to $\Delta T/T$. To do so, we will find first a connection between $\Delta\rho_m/\rho_m$ and $\Delta\rho_r/\rho_r$, and then translate the latter to $\Delta T/T$.

Relating $\Delta\rho_m/\rho_m$ and $\Delta\rho_r/\rho_r$ is easy, since we are dealing with adiabatic perturbations.

We know that: taking differentials

$$\left.\begin{aligned} \rho_m \propto R^{-3} &\Rightarrow \Delta\rho_m \propto -3R^{2}\Delta R = -3\rho_m \frac{\Delta R}{R} \Rightarrow \frac{\Delta\rho_m}{\rho_m} = -3\frac{\Delta R}{R} \\ \rho_r \propto R^{-4} &\Rightarrow \Delta\rho_r \propto -4R^{-3}\Delta R = -4\rho_r \frac{\Delta R}{R} \Rightarrow \frac{\Delta\rho_r}{\rho_r} = -4\frac{\Delta R}{R} \end{aligned}\right\} \quad \boxed{\frac{\Delta\rho_m}{\rho_m} = \frac{3}{4}\frac{\Delta\rho_r}{\rho_r}}$$

Now it is necessary to relate $\Delta\rho_r/\rho_r$ to $\Delta T/T$. This can be done as:

$$\rho_r \propto T^4 \Rightarrow \Delta\rho_r \propto 4T^3\Delta T = 4\frac{\rho_r}{T}\Delta T \longrightarrow \boxed{\frac{\Delta\rho_r}{\rho_r} = 4\frac{\Delta T}{T}}$$

Combining both expressions we find:

$$\boxed{\frac{\Delta T}{T} = \frac{1}{3}\frac{\Delta\rho_m}{\rho_m}}$$

At decoupling, we had $\delta_{m,dec} = \left(\frac{\Delta\rho_m}{\rho_m}\right)_{dec} \gtrsim 10^{-3}$, so $\Delta T/T \approx 10^{-3}$ (and this was a lower limit). Since $\Delta T/T$ remained constant, we should have observed this anisotropies in 1970's and 1980's. However, instead of this we observe is $\Delta T/T \sim 10^{-5}$, two orders of magnitude smaller. To explain this, we need something that starts forming structures before decoupling $\Rightarrow$ The strength of the anisotropies in the CMB is another hint at the existence of dark matter.

Dark matter could form structures prior to recombination. The gravity coupling makes possible to create potential wells to explain the observed $\Delta T/T$.

Thus, the observed $\Delta T/T \approx 10^{5}$ is compatible with $\left(\Delta \rho_m / \rho_m\right)_0 > 1$

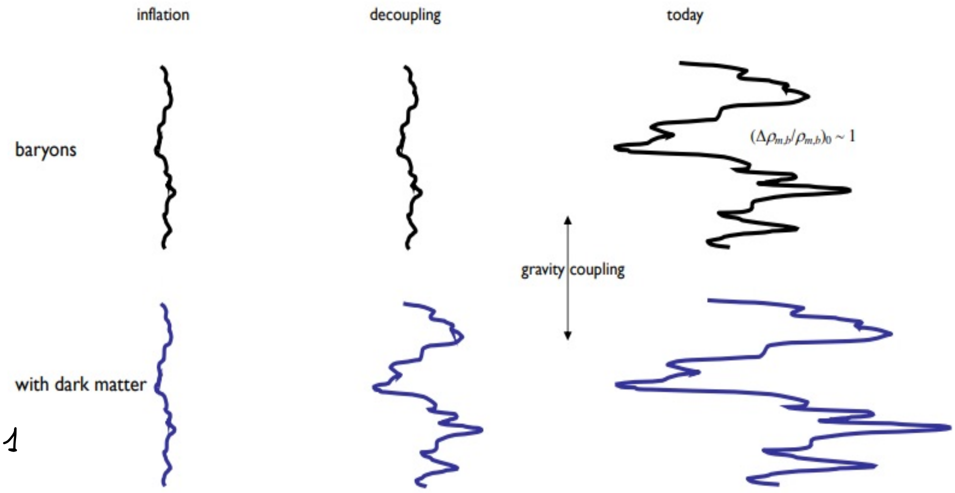

Quantifying fluctuations.

Since we take observations as if we were at the centre of a sphere, the best way of analysing the anisotropies is using the Legendre polynomials, since they are an orthogonal system on spherical coordinates.

We can decompose $\frac{\Delta T}{T}$ as:

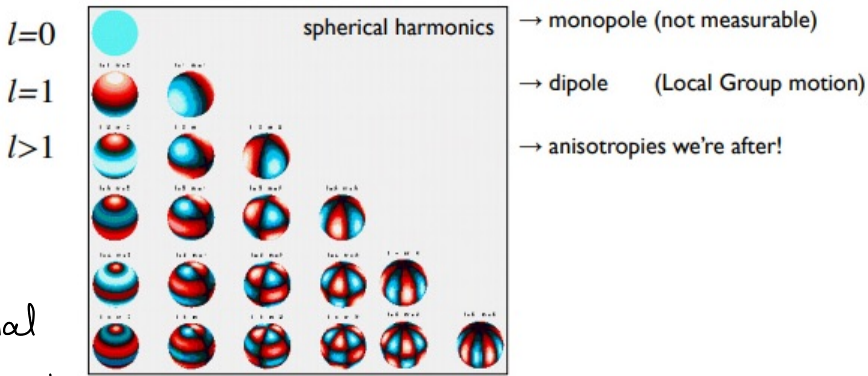

$$\frac{\Delta T}{T}(\theta, \varphi) = \sum_{\ell=0}^{\infty} \sum_{m=-\ell}^{+\ell} a_{\ell m} Y_{\ell m}(\theta, \varphi)$$

$Y_{\ell m}(\theta, \varphi)$: spherical harmonics

Since we have isotropy (i.e., rotational invariance) we can combine the different m-terms:

$$\boxed{C_\ell = \frac{1}{2\ell+1} \sum_{m=-\ell}^{+\ell} |a_{\ell m}|^2}$$

Power spectrum of temperature fluctuations

And define $D_\ell = \frac{1}{2\pi} \ell(\ell+1) C_\ell$

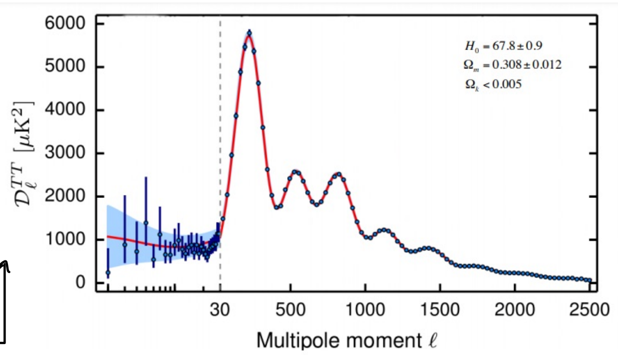

Nature of the fluctuations. Baryonic acoustic oscillations and Sachs-Wolfe effect.

(Baryonic) matter was coupled to radiation prior to $z_{rec} \sim 1330$. The existence of perturbations in the coupled baryons lead to (adiabatic) perturbations in the radiation field. [As we have already calculated, $\delta_b = \frac{3}{4}\delta_r$]. It also leads to baryonic acoustic oscillations. This happens because of the effect of gravity and radiation pressure.

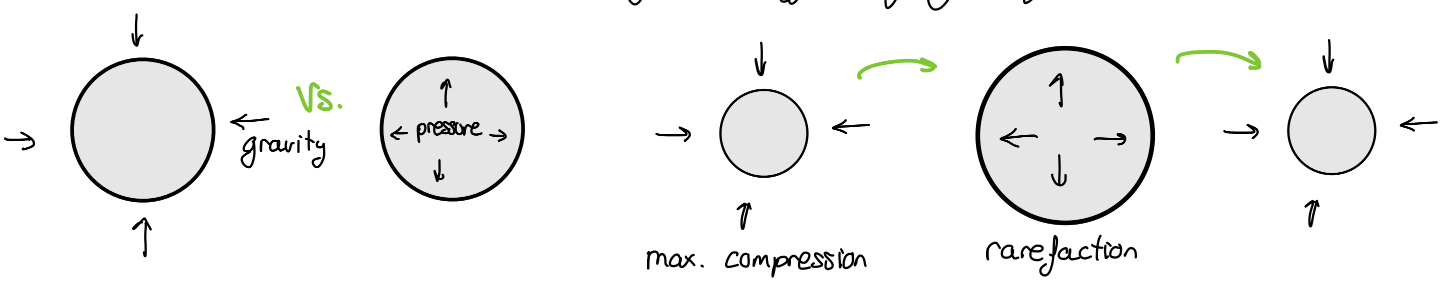

Gravity wants to pull the material inside, but the radiation is exerting a pressure that goes into the other direction that wants to tear things apart. This constant feud generates oscillations.

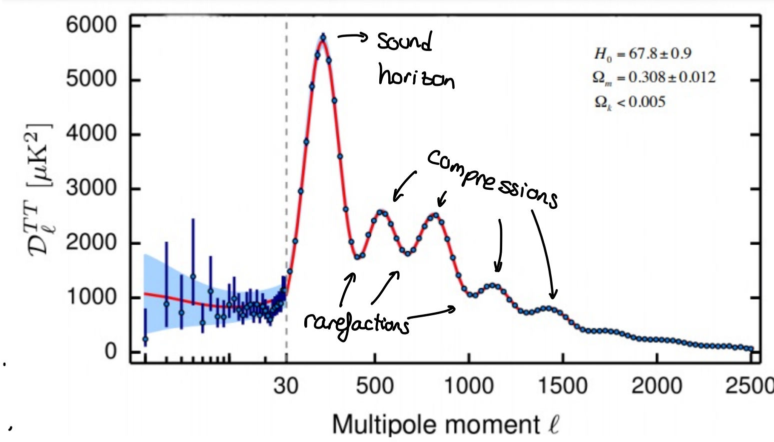

At decoupling this does not happen anymore: oscillations are frozen and photons are caught at extremes.

This translates into temperature fluctuations: we see peaks and dips in the observed $\Delta T/T$.

These are called baryon accoustic oscillations.

Sound waves have an associated speed $c_s = \sqrt{\frac{\partial P}{\partial \rho}} \approx \frac{c}{\sqrt{3}}$

For an overdensity in DM, neutrinos, gas and photons:

- DM is decoupled, and hence able to gravitationally collapse right away (creating gravitational wells).
- Neutrinos are about to decouple and free stream out of the overdensity.
- Gas and photons remain coupled until photon decoupling: we get sound waves, the overdensity/overpressured region travels outwards with $v = c_s$

1
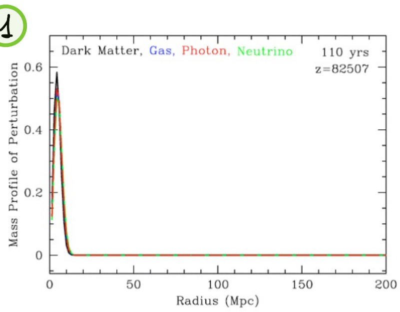

2
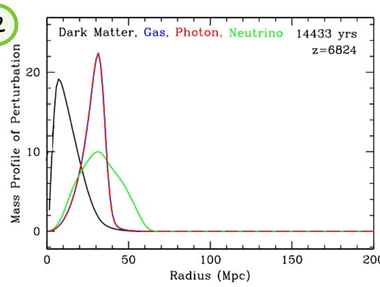

3
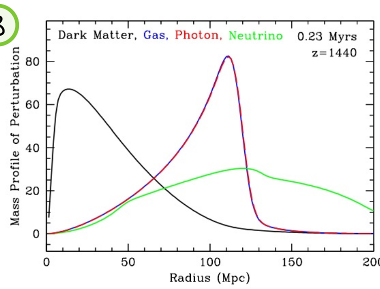

4
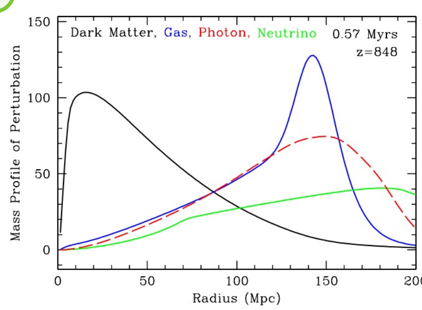

5
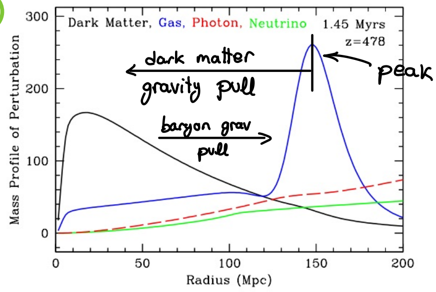

6
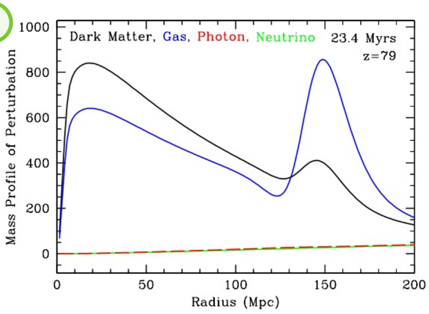

7
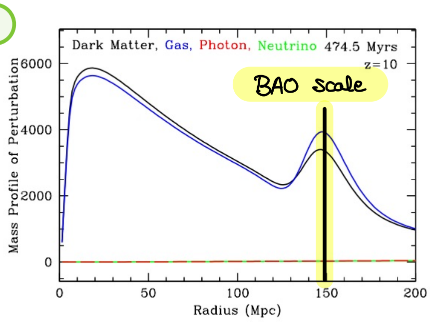

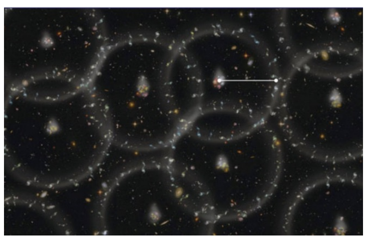

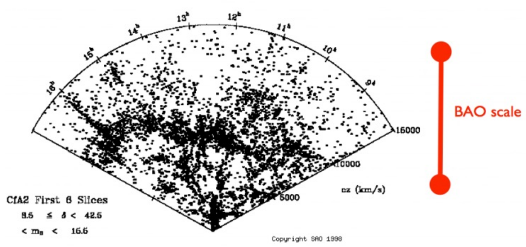

We start when everything is still coupled 1. With the expansion of the universe, gas, photons and neutrinos start to decouple 2. The dark matter is not expanding (it is actually collapsing, since it decoupled a long time ago. Neutrinos are about to decouple as well. Photons and gas are still coupled, so they evolve together. At recombination 3 (+ decoupling) they will start evolving differently 4. Photons and neutrinos evolve on a similar way after they decoupling. There is still a peak for the baryons. That peak now feels the gravity towards the DM peak. If we continue 6, 7, we still have a peak at the size of the horizon at decoupling. This peak should be observable in the Universe (matter overdensity peak) when we look at the distribution of galaxies. To find it, we require for huge surveys to resolve the BAO scale.

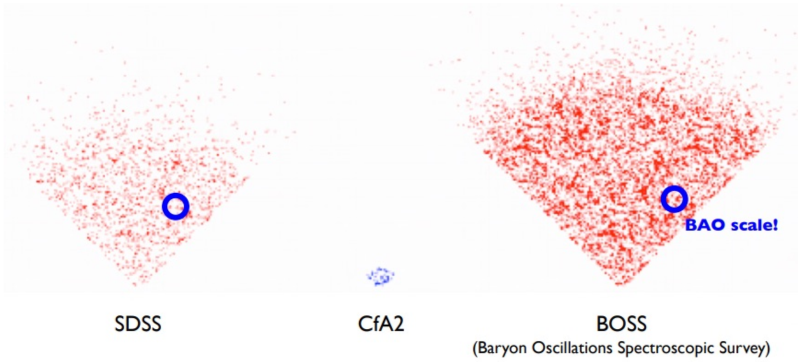

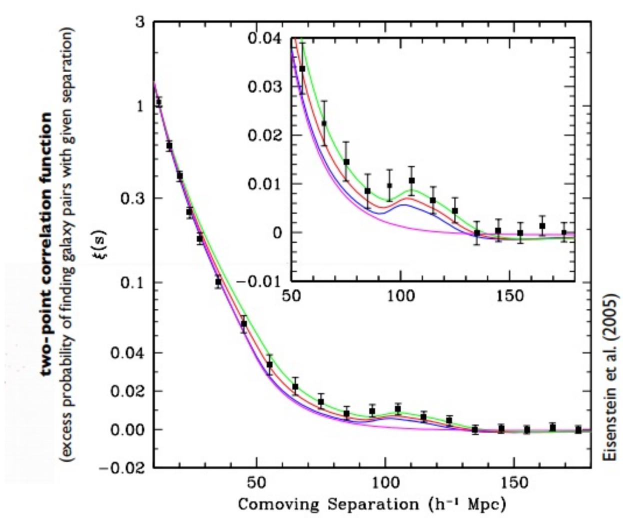

This peak has been found on the distribution of galaxies.

We had found that, for adiabatic fluctuations, the temperature and baryon fluctuations were related as:

because DM is not coupled

$$\frac{\delta T}{T} = \frac{1}{3}\frac{\delta \rho_m}{\rho_m}$$

This fluctuations can be related to the total gravitational potential (which also includes dark matter as:

$$\boxed{\frac{\delta T}{T} = \frac{1}{3}\frac{\delta \Phi}{c^2}}$$

Sachs-Wolfe effect

angular scale of the effect

$$\Delta\Theta \approx 10°$$

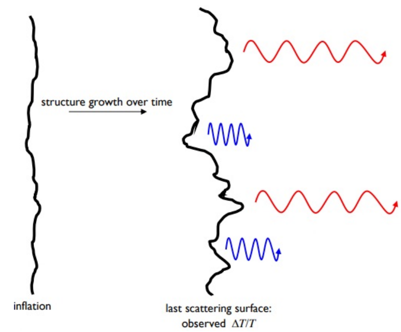

This equation describes the temperature fluctuations in the CMB photons due to the loss in the potential wells created by DM (which was discussed before)

There are other effects that cause some $\delta T/T$, for example, the velocity distribution of the electrons

$$\frac{\delta T}{T} = -\frac{\vec{v}\cdot\vec{n}}{c} \qquad \Delta\theta \approx 1^{\circ}$$

(related to Doppler effect).

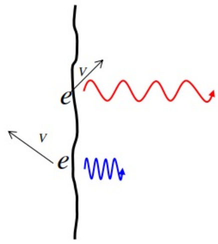

last scattering surface

We also have Silk damping:

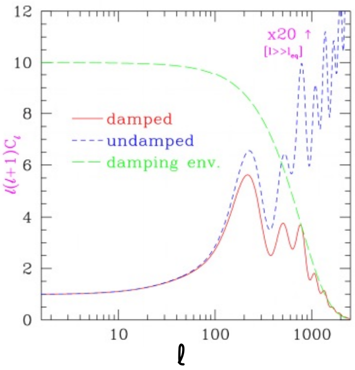

If there were no photon diffusion from high to low-density regions and electrons were not dragged along via Compton interaction, fluctuations would diverge. This, combined with the Coulomb coupling between protons and electrons, damps baryonic density fluctuations on small scales ($\Delta\theta^{\circ} \ll 1$). This damping is sensitive to the baryon content.

Secondary fluctuations

Nature of the fluctuations

This fluctuations appear due to the interaction of CMB photons with matter (e.g. a galaxy cluster) inbetween z_{dec} and $z=0$.

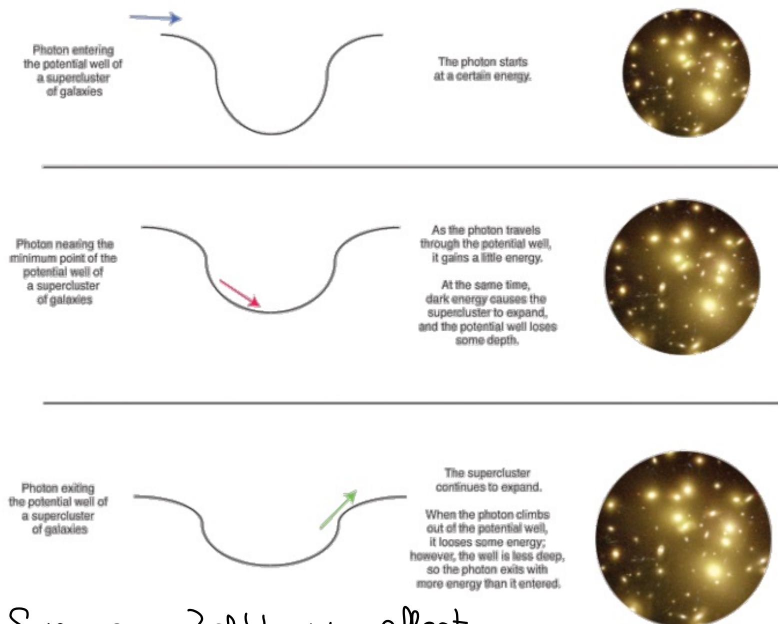

- Integrated Sachs-Wolfe effect

  Fluctuations due to global (time-varying) gravitational potential. They are caused by time-varying linear perturbations (e.g. superclusters)

- Rees - Sciama effect:

  Caused by local (time-varying) gravitational potential. Caused by time-varying non-linear perturbations (e.g. haloes).

- Sunyaev - Zel'dovich effect:

  1. Thermal: CMB photons scatter off the hot intra-cluster gas.
  2. Kinetic: The cluster gas has a bulk motion with respect to the CMB, and hence induces a Doppler shift.

  SZ effect is used to study galaxy clusters.

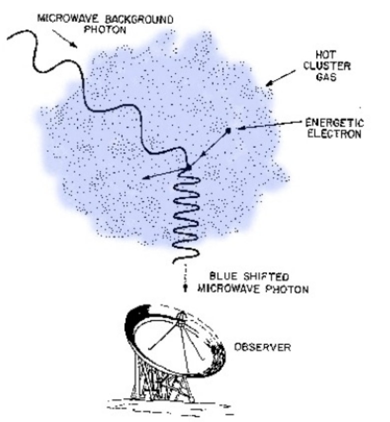

- Ostriker - Vishniac effect

Higher order coupling between bulk flow of electrons and their density perturbation (outside virialized objects).

- Patchy re-ionisation of the Universe : there are HII regions with free e^- for scattering

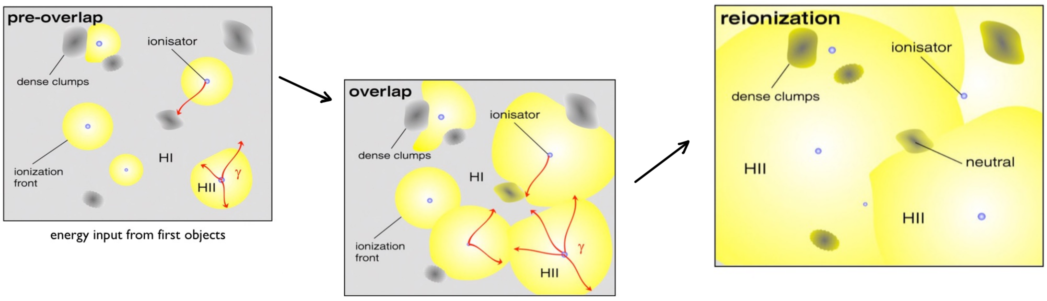

- Gravitational lensing

Importance of secondary anisotropies

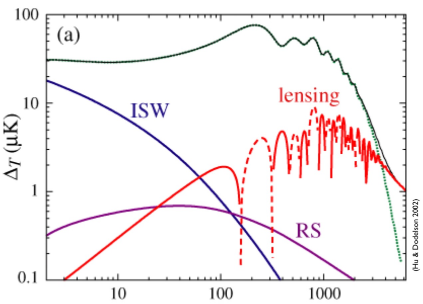

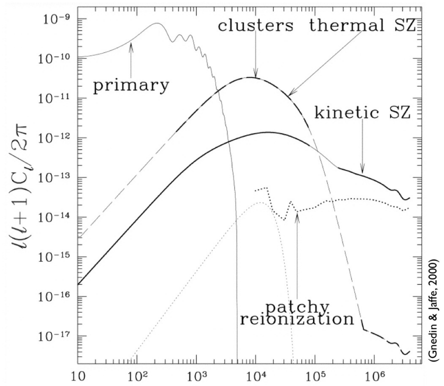

— Primary anisotropies

All the other lines are theoretical calculations of $\delta T/T$ for the secondary effects. These effects are important on very small scales.

For $l > 3000$, lensing and tSZ dominate anisotropies → if we resolve them we can get information about clusters.

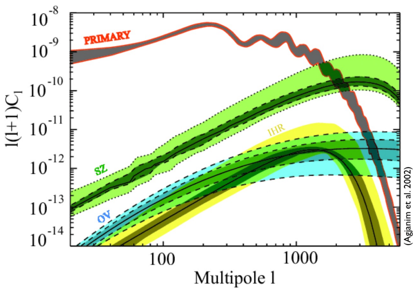

8.4. CMB anisotropies and spectrum

Measurements

We can measure the CMB anisotropies in various frequencies (channels). This variety of channels can be used to substract the Galactic noise. We measure the temperature and polarization of the CMB photons.

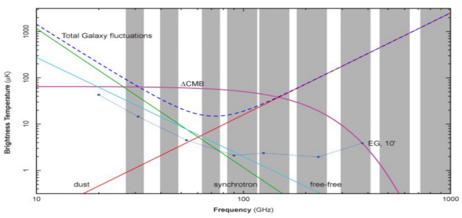

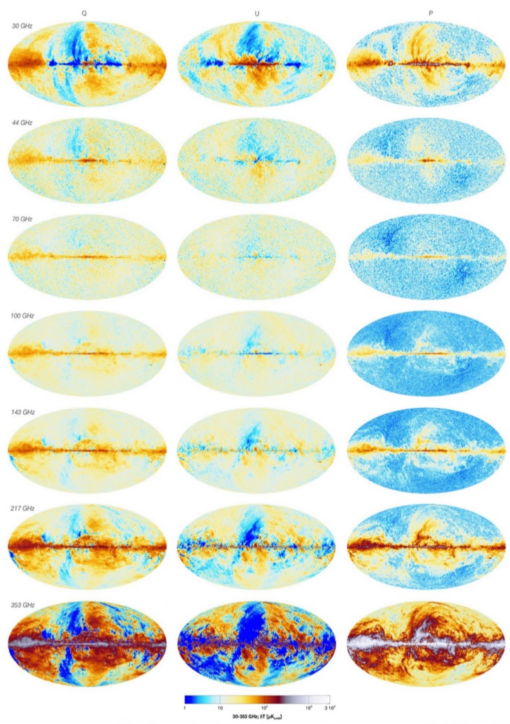

The extra channels also increase resolution, which means that higher multipoles can be measured.

This measures can be translated into C_ℓ (power spectrum)

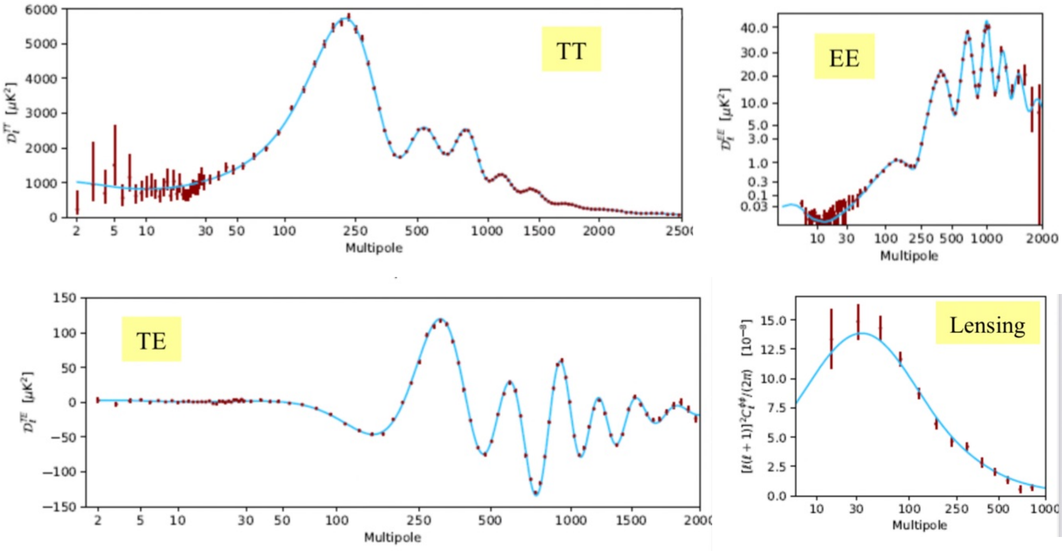

We can split CMB maps into:

- TT: temperature - temperature anisotropy
- TE: temperature - polarization (electric + magnetic)

Oscillations are due to the coupling to baryons (BAO, baryon accoustic oscillations)

CMB data analysis. HEALPix.

As we have discussed before, we can analyse the CMB temperature fluctuations expanding on Legendre polynomials and spherical harmonics

$\Delta \equiv \Delta T/T$ ⟵ Temperature anisotropy (the CMB map)

Fourier ; expand in Legendre ; Legendre polynomials

$$\Delta(\vec{x}, \hat{n}, \tau) = \int d^3k\, e^{i\vec{k}\cdot\vec{x}}\, \Delta(\vec{k}, \hat{n}, \tau) \equiv \int d^3k\, e^{i\vec{k}\cdot\vec{x}} \sum_{\ell=0}^{\infty} (-i)^\ell (2\ell+1)\, \Delta_\ell(\vec{k}, \tau)\, P_\ell(\hat{k}\cdot\hat{n})$$

$$\Delta(\hat{n}) = \sum_{\ell=0}^{\infty} \sum_{m=-\ell}^{\ell} a_{\ell m}\, Y_{\ell m}(\hat{n}) \qquad a_{\ell m} = (-i)^\ell 4\pi \int d^3k\, Y^*_{\ell m}(\hat{k})\, \Delta_\ell(\vec{k}, \tau)$$

↳ spherical harmonics

This is done because it is more efficient to work with spherical harmonics than with the pixels, which allows us to reduce the computational weight without losing information.

NOTE

- Properties of the Legendre polynomials

$$\int_{-1}^{1} dx\, P_\ell(x)\, P_{\ell'}(x) = \delta_{\ell\ell'} \frac{2}{2\ell+1}$$ ↙ orthogonality

$$P_0(x) = 1 \qquad P_1(x) = x \qquad -1 < x < 1 \qquad P_2(x) = \frac{3x^2-1}{2}$$

$$(\ell+1) P_{\ell+1}(x) = (2\ell+1)\, x\, P_\ell(x) - \ell P_{\ell-1}(x)$$

- Properties of the Spherical harmonics

$$\int d\Omega\, Y^*_{\ell m}(\Omega)\, Y_{\ell' m'}(\Omega) = \delta_{\ell\ell'}\delta_{mm'} \longrightarrow P_\ell(\hat{x}\cdot\hat{x}') = \frac{4\pi}{2\ell+1} \sum_{m=-\ell}^{\ell} Y_{\ell m}(\hat{x})\, Y^*_{\ell m}(x')$$

$$Y_{00}(\theta, \phi) = \frac{1}{\sqrt{2\pi}}$$

$$Y_{1,\pm1}(\theta, \phi) = \mp i \sqrt{\frac{3}{8\pi}} \sin(\theta)\, e^{\pm i\phi}$$

We are not interested in the temperature anisotropy itself, we are interested on the two-point correlation function for the temperature anisotropy:

$$C(\theta) \equiv \langle \Delta(\hat{n}_1)\, \Delta(\hat{n}_2) \rangle = \frac{1}{4\pi} \sum_{\ell=0}^{\infty} (2\ell+1)\, C_\ell\, P_\ell\, (\hat{n}_1 \cdot \hat{n}_2)$$

Considering the properties writen above, we have:

$$\langle a_{\ell m}\, a^*_{\ell' m'} \rangle = C_\ell\, \delta_{\ell\ell'}\, \delta_{mm'}$$

Decomposing also the Fourier transform of the temperature anisotropy:

$$\Delta_\ell(\vec{k}, z) = \Psi_i(\vec{k})\, \Delta_\ell(k, T) \longrightarrow \langle \Psi_i(\vec{k}_1)\, \Psi_i(\vec{k}_2) \rangle = P_\Psi(k)\, \delta_D(\vec{k}_1 + \vec{k}_2)$$

↳ initial perturbation (from inflation) ↳ Primordial power spectrum

Puting everything together, it is possible to calculate the C_ℓs as:

$$\boxed{C_\ell = 4\pi \int d^3k\, P_\Psi(k)\, \Delta_\ell^2(k, z)}$$

$P_\Psi(k) \rightarrow$ Primordial power spectrum

$\Delta_\ell \rightarrow$ Legendre expansion of the F.T. of the T anisotropy

The C_ℓs compress information: From 5×10^7 px ($n_{side} = 2048$, $n_{pix} = 12 \times n_{side}^2$) to ~ 2500 multipoles.

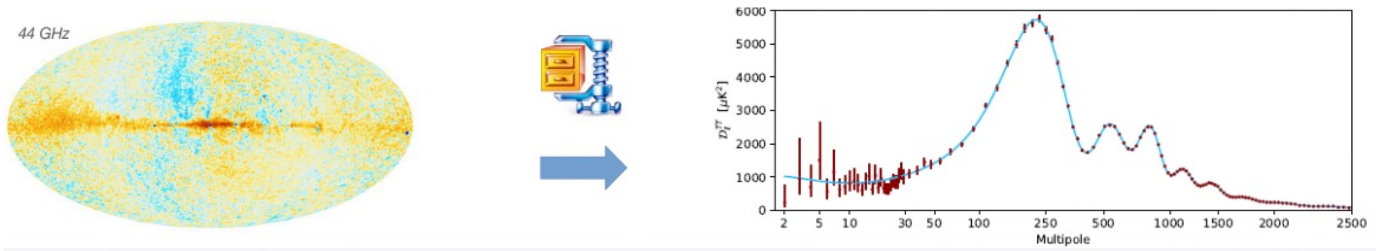

HEALPix

(Hierarchical Equal Area isoLatitude Pixelisation). A 2-sphere is tesselated into curvilinear quadrilaterals with different resolutions. The lowest one has 12 pixels, and the resolution is increased partitioning every pixel into 4 new.

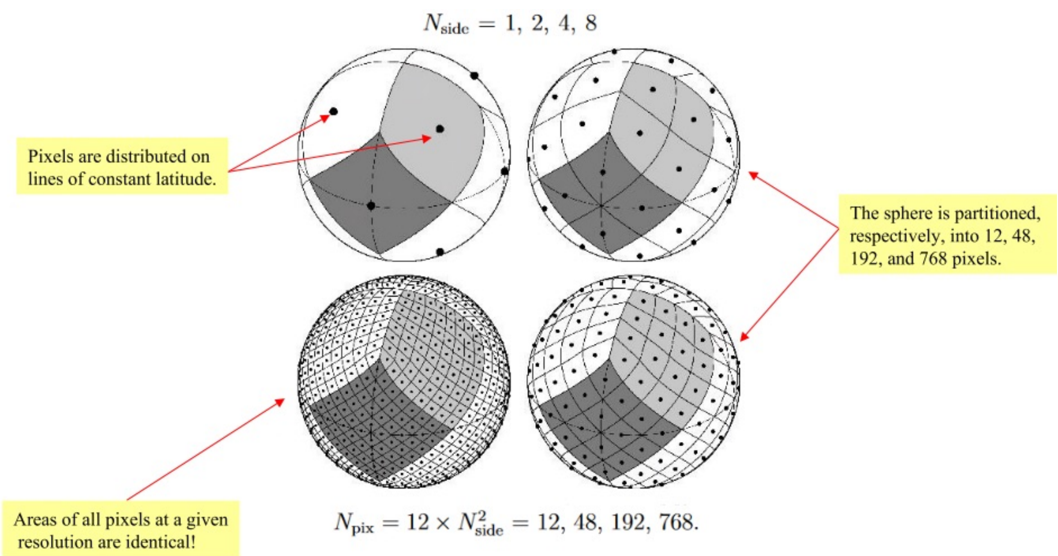

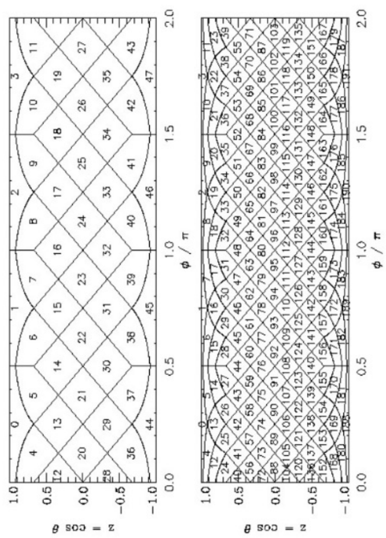

Plane projection

If the intensity (or temperature) of the photons is known in every pixel, we can obtain:

$$\hat{a}_{\ell m} = \frac{4\pi}{N_{pix}} \sum_{p=0}^{N_{pix}-1} \underbrace{Y^{*}_{\ell m}(\gamma_p) f(\gamma_p)}_{\text{complex number}} \longrightarrow \underbrace{\hat{C}_\ell}_{\text{real number}} = \frac{1}{2\ell+1} \sum_m |\hat{a}_{\ell m}|^2$$

It is necessary to know the angles associated to each pixel.

CMB polarization modes

Until now, we were talking about temperature fluctuations, but it is also possible to measure the polarization from Thomson scattering (E and B modes).

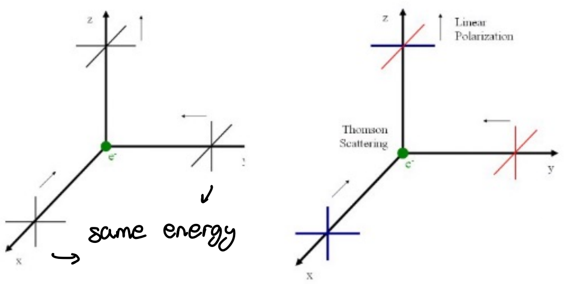

Photons coming from the x and y axis will be scattered by the electron at the origin, adquiring some polarization in the z direction (normal to the direction of motion, all the other information is lost due to the Thomson scattering).

Photons with different energies (i.e. coming from regions with different matter densities) will produce differences on the polarization after the scatter (mixed signal on the different axis).

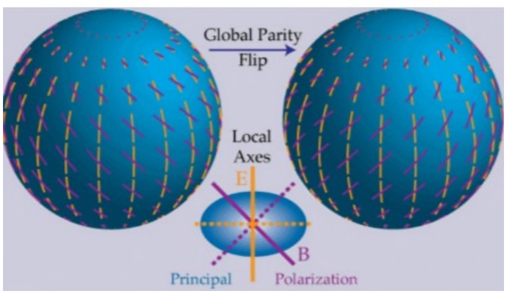

This signal can be decomposed in Electric and Magnetic parts (convention).

The E mode is caused by thermal over/under-densities.

B mode is caused by GW and dust (due to magnetic fields and imperfect alignment).

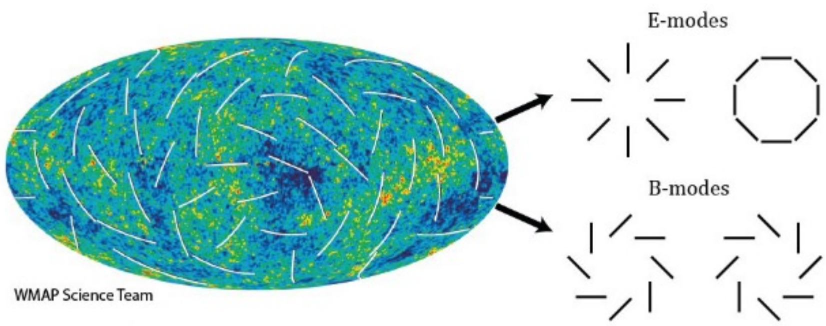

8.5. Features of the TT CMB spectrum

We have already discussed qualitatively some of the features of the CMB Power spectrum (like baryonic accoustic oscillations), but now we are taking a deeper look into it.

For now, we will only pay attention to the TT power spectrum. Some of the outstanding features are:

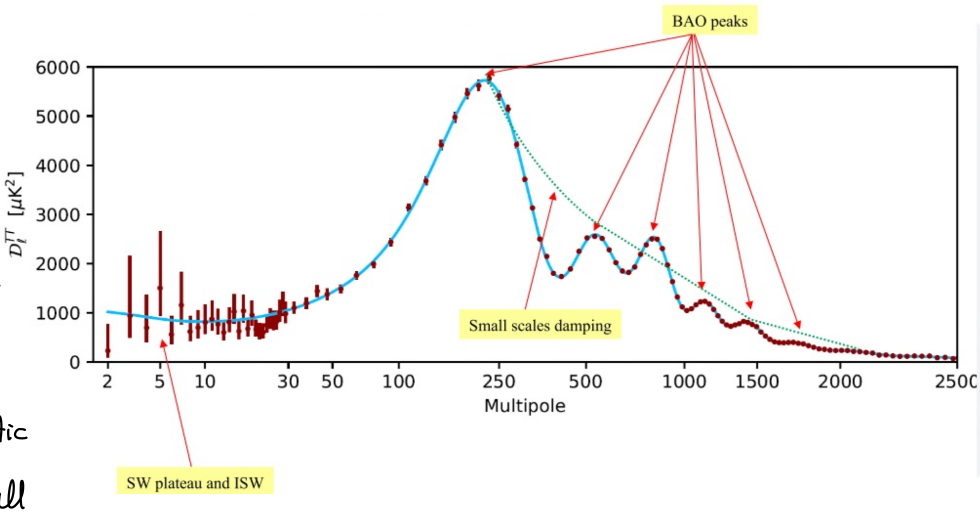

- Plateau for large scales (SW + ISW, flat C_ℓs for $\ell < 30$)
- BAO peaks - baryonic accoustic oscillations, damped for small scales (diffusion damping, due to an increase in mean free path of photons).

There are also some other effects, like:

- Adiabatic/isocurvature perturbations
- Doppler shift

} (primary anisotropies - before last scattering surface)

- Integrated Sachs-Wolfe effect (ISW)
- Reionization at $z = 10$

} (secondary anisotropies - after CMB emision)

Baryon accoustic oscillations

We have coupled photons and baryons inside a potential well. We must solve the fluid equations for both components. To do so, we can use the following perturbation equations for Baryon-Photon plasma:

Metric perturbations, Newtonian potentials

Thomson cross section

$$\dot{\delta}_\gamma = -\frac{4}{3}\theta_\gamma + 4\dot{\phi}$$

$$\dot{\theta}_\gamma = k^2\left(\frac{1}{4}\delta_\gamma - \sigma_\gamma\right) + k^2\psi + a n_e \sigma_T (\theta_b - \theta_\gamma)$$

Isotropic stress

$$\dot{\delta}_b = -\theta_b + 3\dot{\phi}$$

$$\dot{\theta}_b = -\frac{\dot{a}}{a}\theta_b + c_s^2 k^2 \delta_b + \frac{4\bar{\rho}_\gamma}{3\bar{\rho}_b} a n_e \sigma_T (\theta_\gamma - \theta_b) + k^2\psi$$

NOTATION

$\delta \equiv \Delta\rho/\rho$ → Density perturbations of photons / baryons

$\theta = i k^j v_j$ → Velocity perturbation

Without the $(\theta_b - \theta_\gamma)$ term, the equations would be decoupled and there would be no BAO.

To solve them analytically, we can define S as:

$$\delta_\gamma - 4\phi \equiv 4S$$

And elliminate all except δ_γ

$$\ddot{S} + \underbrace{\frac{\dot{R}}{1+R}}_{\text{damping term}}\dot{S} + \underbrace{k^2 c_s^2 S}_{\text{oscillatory term}} = \overbrace{\left(-\frac{k^2}{3}\psi - \frac{k^2}{3}\frac{\phi}{1+R}\right)}^{\text{driving force}}$$

R → Ratio Ω_b/Ω_γ, will be defined later

To get an initial approximation to the behavior of the solution, we can consider the zero order solution (ignoring the damping and force):

$$\ddot{S} + k^2 c_s^2 S \simeq 0 \longrightarrow S = A\cos(k r_s + \Theta_0)$$

where $r_s = \int_0^{\eta} d\eta' \, c_s(\eta') \simeq c_s(\eta)\,\eta$ (sound horizon)

$$c_s^2 = \frac{1}{3(1+R)}$$ — sound speed of the baryon-photon plasma

$$R = \frac{3}{4}\frac{\Omega_b}{\Omega_\gamma} = \frac{a^{-3}}{a^{-4}} R_0 = R_0 a$$

Comparing the position of the peaks:

$$k_p = \frac{n\pi}{r_s}$$

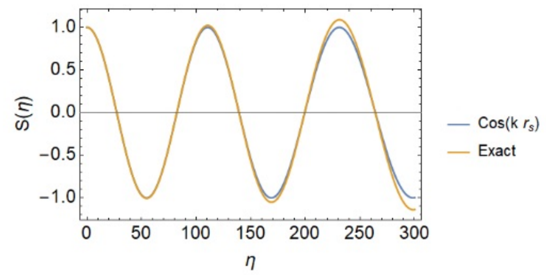

A more careful calculation yields:

$$\ell_A \equiv \pi D / s_*$$

$$\ell_A \approx 172\, d \left(\frac{z_*}{10^3}\right)^{1/2} \left(\frac{1}{\sqrt{R_*}} \ln \frac{\sqrt{1+R_*} + \sqrt{R_* + r_* R_*}}{1 + \sqrt{r_* R_*}}\right)^{-1}$$

where D is the distance to the sound horizon (recombination), ℓ_A is the multipole of the spectrum, s is the sound horizon.

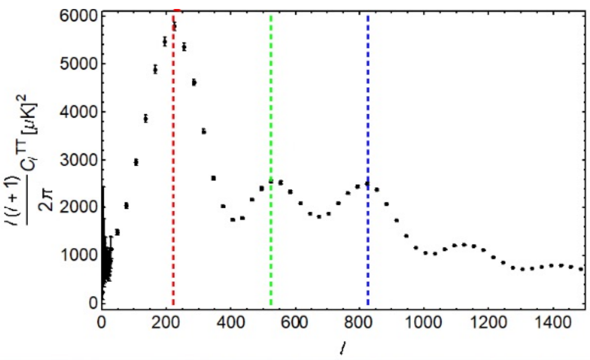

The peaks are located at:

$$\boxed{\begin{aligned} \ell_m &= \ell_A (m - \phi) \\ \phi &\approx 0.267 \left(\frac{r_*}{0.3}\right)^{0.1} \end{aligned}}$$

$m \equiv$ number of the peak

Hot and Cold spots

Photons going through overdense or underdense regions of the Universe will change their T. To calculate this, we consider the perturbed FRW metric with Newtonian potentials φ, Ψ.

$$ds^2 = a^2(\tau)\{-(1+2\Psi)\,d\tau^2 + (1-2\phi)\,dx^i dx_i\}$$

The Photon four momentum, given the FRW metric:

$$P^\mu = \left(a^{-1} p (1-\Psi),\ a^{-1} p^i (1+\phi)\right) \xrightarrow{\text{temporal part}} P^0 = a^{-1} p (1-\Psi) \sim \frac{1}{\lambda}$$

Einstein equations (0,0) and (i,j) parts give Poisson equations:

$$\left.\begin{aligned} k^2 \phi &= -4\pi G_N a^2 \rho_m \delta_m \\ \phi &= \Psi \end{aligned}\right\} \Psi = -4\pi G_N \frac{a^2}{k^2} \rho_m \delta_m$$

↳ Ψ is related to the DM density perturbations.

δ is the density contrast, defined as $\delta = (\rho - \bar\rho)/\bar\rho$. We can define over/under densities as: $\delta_{over} \gg (\delta_{average}) \gg \delta_{under}$

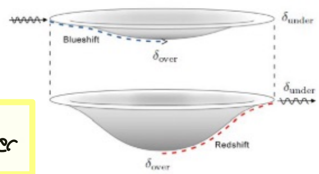

This translates into redshift for photons trying to escape:

$$\boxed{\delta_{over} > \delta_{under} \longrightarrow \Psi_{over} < \Psi_{under} \longrightarrow P^0_{over} > P^0_{under} \longrightarrow \lambda_{over} < \lambda_{under}}$$

↑ photon energy

This leads to temperature decreases (coldspot) between overdensity and underdensity:

$$\boxed{\frac{\Delta T}{T} \sim \frac{1}{3}\delta\Psi} \longrightarrow \frac{\Delta T}{T} < 0$$

$\Delta T = T_{over} - T_{under}$

$\delta\Psi = \Psi_{over} - \Psi_{under} < 0$

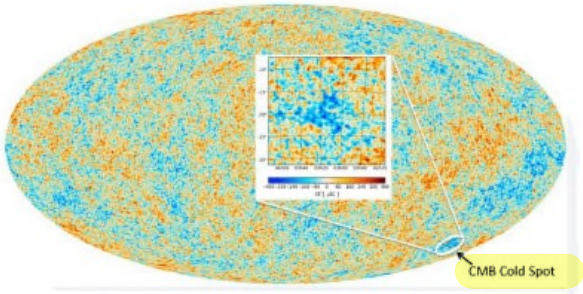

For some reason, that region is colder

Derivation of Sachs-Wolfe effect

Scalar perturbations

It appears when a photon escapes a static potential. Since $\frac{\Delta T}{T} \sim \frac{1}{3}\delta\Psi$, it is important on large scales. To zero order, the SW effect contribution is a spherical Bessel function (see Dodelson 8.6).

Legendre expansion coefficient

Bessel function

$$\Theta(\hat{n}, \tau_0) \approx \frac{1}{3}\Psi(\vec{x} = -\vec{n}\chi, \tau_{rec}) \longrightarrow \Theta_\ell(k, \tau) = \frac{1}{3} j_\ell(k\chi)$$

If we assume that the spectrum from inflation is a Power Law:

$$P_\Psi(k) = A\chi^3 (k\chi)^{n-4} \propto k^{n-4}$$

The coefficients give:

$$\boxed{\begin{aligned} C_\ell &\approx \frac{2^n \pi^3}{9} A \frac{\Gamma(3-n)\,\Gamma\left(\frac{2\ell+n-1}{2}\right)}{\Gamma^2\left(\frac{4-n}{2}\right)\Gamma\left(\frac{2\ell+5-n}{2}\right)} \\ n=1: \quad C_\ell &\approx \frac{8\pi^2}{9}\frac{A}{\ell(\ell+1)} \longleftarrow \text{constant} \end{aligned}}$$

Some people use different notations that give some extra factors, but they can be re-absorbed in the amplitude:

$$C(\theta) = \left\langle \frac{\delta T^*}{T}(\vec{n}) \frac{\delta T}{T}(\vec{n}') \right\rangle_{\vec{n}\cdot\vec{n}' = \cos\theta} = \frac{1}{4\pi}\sum_{\ell=2}^{\infty}(2\ell+1) C_\ell P_\ell(\cos\theta)$$

$$\frac{\delta T}{T}(\theta,\phi) = \frac{1}{3}\Phi(\eta_{ls}) Q = \frac{1}{5}\mathcal{R} Q(\eta_0, \theta, \phi) \equiv \sum_{\ell=2}^{\infty}\sum_{m=-\ell}^{\ell} a_{\ell m} Y_{\ell m}(\theta,\phi)$$

$$\hookrightarrow \Phi = \frac{3}{5}\mathcal{R}$$

$$C_\ell^{(S)} = \frac{4\pi}{25}\int_0^\infty \frac{dk}{k} P_{\mathcal{R}}(k)\, j_\ell^2(k\eta_0) \longrightarrow C_\ell^{(S)} = \frac{2\pi}{25} A_S^2 \frac{\Gamma[\frac{3}{2}]\,\Gamma\left(1-\frac{n-1}{2}\right)\Gamma\left(\ell+\frac{n-1}{2}\right)}{\Gamma\left(\frac{3}{2}-\frac{n-1}{2}\right)\Gamma\left(\ell+2-\frac{n-1}{2}\right)}$$

$$\frac{\ell(\ell+1)C_\ell^{(S)}}{2\pi} = \frac{A_S^2}{25} = \text{constant} \quad \text{for } n=1$$

The amplitude is more or less constant because the fourier modes have not entered the horizon yet (large scales). The perturbations are frozen, they are outside any causal contact. They still have the primordial values from inflation.

Tensor perturbations

Tensor perturbations follow the following ODE:

$$h_k'' + 3\mathcal{H} h_k' + (k^2 + 2K) h_k = 0$$

The contribution in the spectrum is:

$$\frac{\delta T}{T}(\theta, \phi) = \int_{\eta_{LS}}^{\eta_0} dr\, h'(\eta_0 - r)\, Q_{rr}(r, \theta, \phi) \qquad Q_{k\ell}^{rr}(r) = \left[\frac{(\ell-1)\ell(\ell+1)(\ell+2)}{\pi k^2}\right]^{1/2} \frac{j_\ell(kr)}{r^2}$$

We can calculate the C_ℓs as:

$$C_\ell^{(T)} = \frac{9\pi}{4}(\ell-1)\ell(\ell+1)(\ell+2)\int_0^\infty \frac{dk}{k} P_g(k)\, I_{k\ell}^2 \qquad I_{k\ell} = \int_0^{x_0} dx \frac{j_2(x_0 - x)\, j_\ell(x)}{(x_0 - x)\, x^2}$$

And again, for large scales (small multipoles):

$$\ell(\ell+1) C_\ell^{(T)} = \frac{\pi}{36}\left(1 + \frac{48\pi^2}{385}\right) A_T^2 B_\ell$$

$B_\ell = (1.1184,\ 0.8789, \dots, 1.00)$ for $\ell = 2, 3, \dots, 30$

The Integrated Sachs-Wolfe effect

ISW appears when photon escapes time varying potential due to accelerated expansion caused by dark energy. It appears at late times at large scales ($\ell < 20$)

$$\frac{\Delta T}{T} \simeq \int_0^{\eta_0} (\dot\phi + \dot\psi)\, d\eta \xrightarrow{\text{expansion}} \Delta_\ell \simeq \int_0^{\eta_0} e^{-\tau}(\dot\phi + \dot\psi)\, j_\ell[k(\eta_0 - \eta)]\, d\eta$$

$$\tau = \int_{\eta_{rec}}^{\eta_0} d\eta\, n_e \sigma_T\, a(\eta) \quad \text{- optical depth}$$

The C_ℓs strongly depend on DE:

$$C_\ell^{ISW} = 4\pi \int \frac{dk}{k} I_\ell^{ISW}(k)^2 \frac{9}{25} \frac{k^3 P_\zeta}{2\pi^2}$$

$$\frac{k^3 P_\zeta}{2\pi^2} = A_s \left(\frac{k}{k_0}\right)^{n_s - 1} T(k)^2$$

Transfer function

$$I_\ell^{ISW}(k) = 2\int dz \frac{dG}{dz} j_\ell(k r(z))$$

$$G(a,k) = \frac{\Phi(a,k) + \Psi(a,k)}{\Phi(a_{ini},k) + \Psi(a_{ini},k)}$$

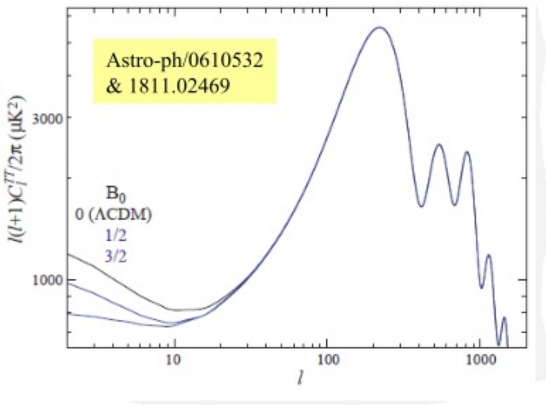

However, for small multipoles we have a problem with cosmic variance. There are few m coefficients, so the errors are large.

Other effects

Diffusion damping

Damping at small scales (large ℓ) due to an increase in the mean free path of photons

$$\ddot{\delta} + \frac{\dot{R}}{1+R}\dot{\delta} + k^2 c_s^2\,\delta = \left(-\frac{k^2}{3}\psi - \frac{k^2}{3}\frac{\phi}{1+R}\right)$$

$k^2 c_s^2\,\delta$ ↳ oscillatory term

$\left(-\frac{k^2}{3}\psi - \frac{k^2}{3}\frac{\phi}{1+R}\right)$ ↳ driving force

$\frac{\dot{R}}{1+R}\dot{\delta}$ ↳ damping term

The damping term gives rise to an exponential suppression in C_ℓs. (Dodelson 8.4)

$$\delta_\gamma \simeq \cos\left(k r_s(\eta)\right) e^{-k^2/k_D^2}$$

$$k_D^{-2} \equiv \int_0^\eta \frac{d\eta'}{6(1+R) n_e \sigma_T a(\eta')}\left[\frac{R^2}{1+R} + \frac{8}{9}\right] \rightarrow$$ Because we want an integrated effect for all times

Adiabatic / isocurvature perturbations

Until now, we were not considering which kinds of perturbations were we dealing with. Considering a volume with equal distribution of matter and radiation, it can be perturbed in two ways:

i) Change volume adiabatically (conserving the entropy) → the number density is the same

$$\delta_\gamma = \frac{\delta\rho_\gamma}{\rho_\gamma} = \frac{\delta n_\gamma}{n_\gamma} \xrightarrow{n_\gamma \sim T^3} \frac{\delta T}{T} = \frac{\delta_\gamma}{3} \longrightarrow \delta_\gamma = 3\frac{\delta T}{T}$$

ii) Perturb entropy, keep energy density the same (isocurvature): $\rho_m \delta_m = \rho_\gamma \delta_\gamma$

$$\delta_\gamma = 3\frac{\delta T}{T} + \text{const}$$

const ↳ extra correction

This kinds of perturbations have been included in codes, which show that the adiabatic ones are prefered.

Dopler shift (dipole):

Plasma had non-zero velocity at recombination, and the Milky Way moves at 600 km/s w.r.t. the CMB. This produces a dipole (first multipole).

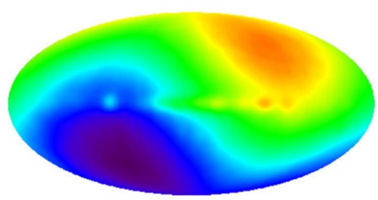

$$\frac{\delta T}{T}(\vec{r}) = -\frac{\vec{r}\cdot\vec{v}}{c}$$

Reionization at $z \sim 10$.

From quasar spectra, we know that the Universe reionized at $z \sim [6,20]$. These electrons scattered again CMB photons, affecting modes within the horizon at the time of reionization, $\ell >> 1$ (small scales) by reducing the C_ℓs: $\Delta_\ell \longrightarrow \Delta_\ell e^{-2}$ $\quad \tau = \int_{\eta_{rec}}^{\eta_0} d\eta\, n_e \sigma_T a(\eta)$

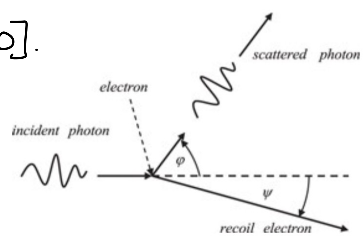

Cosmic variance

For each ℓ we have $2\ell+1$ $a_{\ell m}$ coefficients, of which we can only predict the distribution, not actual values (they are random values).

$\ell = 100 \rightarrow 201\ a_{\ell m}$ (good for statistics)

$\ell = 2 \rightarrow 5\ a_{\ell m}$ (not good for stat)

$$a_{\ell m} = (-i)^{\ell} 4\pi \int d^3k\, Y^*_{\ell m}(\hat{k})\, \Delta_\ell(\vec{k}, \tau)$$

$$\langle a_{\ell m} a^*_{\ell' m'} \rangle = C_\ell\, \delta_{\ell\ell'}\, \delta_{mm'}$$

Sensitivity to cosmological parameters

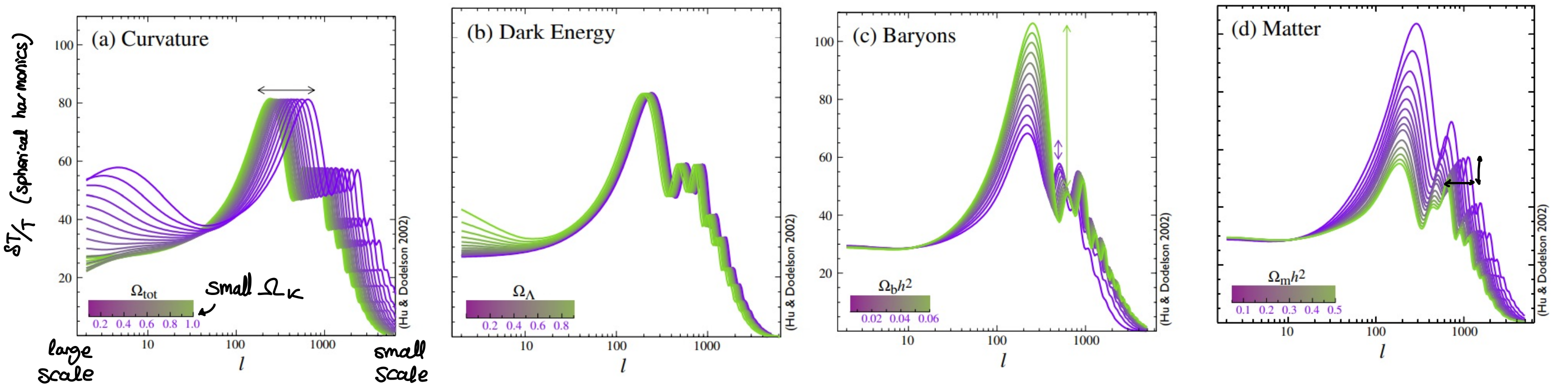

Taking our typical decomposition in spherical harmonics of $\delta T/T$ characterized by their ℓ (scale), we can find the dependences on the position of the peaks with the cosmological density parameters.

a) Curvature does not change the shape of the spectrum, but shifts the position of the peaks. We have measured the first peak on $\ell = 200$, which means that the universe is almost flat.

c) Changing the baryon content modifies the difference between the height of the first and the second peak.

d) Changing all the matter content changes mostly the height of the third peak and its position.

b) Λ has a similar effect than K

NOTE

Anisotropies primarly depend on baryon-photon interactions - ratio

Dark matter has decoupled long before the emergence of the anisotropies

> The shape of the power spectrum of the intrinsic temperature fluctuations in the CMB depends sensitively on the cosmological parameters.

Curvature

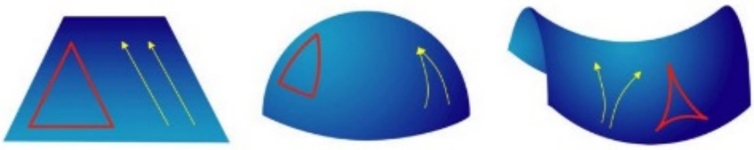

Curvature changes distances:

$$d_A = \frac{1}{1+z}\,\frac{c}{H_0\sqrt{\Omega_K^{(0)}}}\,\sinh\left(\sqrt{\Omega_K^{(0)}}\int_0^z \frac{d\tilde{z}}{E(\tilde{z})}\right)$$

Its main effect is on the location of the 1st peak (~ distance to recombinaton). As it was discussed before, the location of the peaks is given by: $\ell_m = \ell_A(m-\phi)$, $\ell_A \propto D$,
$\phi \approx 0.267\left(r_*/0.3\right)^{0.1}$

Spectral index

The spectral index n_s affects normalization

$$C_\ell = 4\pi\int d^3k\; P_\varphi(k)\,\Delta_\ell^2(k,\tau) \xrightarrow{\text{Taylor}} \frac{C_\ell(n_s)}{C_\ell(n_s=1)} \simeq \left(\frac{\ell}{\ell_0}\right)^{n_s-1}$$

$$P_\varphi \sim k^{n_s-1}$$

Dark energy

It has a late time effect ($z<1$) at large scales ($\ell<10$) [Integrated SW]

$$C_\ell^{ISW} = 4\pi\int\frac{dk}{k}\,I_\ell^{ISW}(k)^2\,\frac{9}{25}\,\frac{k^3P_\varphi}{2\pi^2} \qquad I_\ell^{ISW}(k) = 2\int dz\,\frac{dG}{dz}\,j_\ell(k\,r(z))$$

It also changes the distance to recombination, since it is changing slightly the expansion velocity.

Matter content Ω_m

Ω_m affects the DM potentials. Deeper potentials imply less BAO.

$$\Psi = -4\pi G_N\frac{a^2}{k^2}\rho_m\,\delta_m$$

Baryon content Ω_b

Ω_b affects the height of the peaks.

$$\ddot{S} + \frac{\dot{R}}{1+R}\dot{S} + k^2c_s^2S = \left(-\frac{k^2}{3}\psi - \frac{k^2}{3}\frac{\phi}{1+R}\right)$$

$$R = \frac{3}{4}\frac{\Omega_b}{\Omega_\gamma} = \frac{a^{-3}}{a^{-4}}R_0 = R_0\,a \longrightarrow \text{Amplitude, appears in the driving force}$$

Curvature

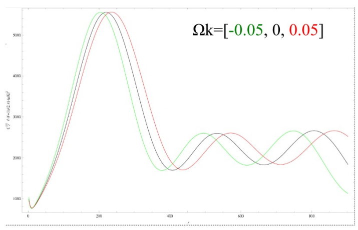

Dark energy

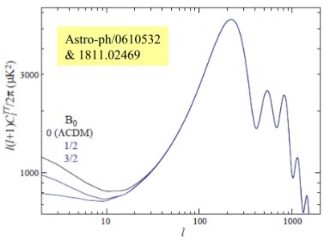

Dark matter

Ωm=[0.2038, 0.2538, 0.3038] and H0=70
Ωmh^2=[0.099862, 0.124362, 0.148862]

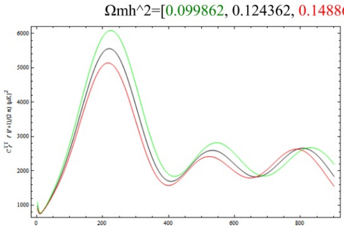

Baryons

Ωb=[0.0362, 0.0462, 0.0562] and H0=70
Ωbh^2=[0.017738, 0.022638, 0.027538]

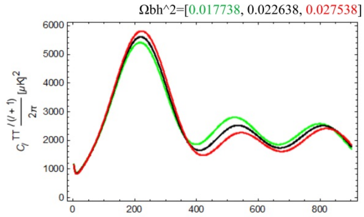

Behaviour of the Power spectrum

The matter power spectrum is the expectation value of the dark matter density perturbations:

$P(k) = \langle |\delta_k|^2 \rangle$

BEWARE
It is not the same of the P_Φ that we had before. P_Φ is the power inflation from inflation.

It is an important quantity that implicitely affects the CMB. The PS can tell us what is happening with the perturbations and how can they affect the CMB. If we take the potential, we can decompose it into:

$$\Phi(k,a) = \Phi_p(k) \times T(k) \times \delta(a)$$

$\delta(a)$ → Matter density contrast

$T(k)$ → Transfer function (normalization)

$\Phi_p(k)$ → Initial value from inflation

$\langle \Phi_p^2 \rangle \sim k^3 k^{n_s - 1}$

$$T(k) = \frac{\Phi(k, a_{late})}{\Phi_{large}(k, a_{late})}$$

Difference in the potentials between any scale and large scale

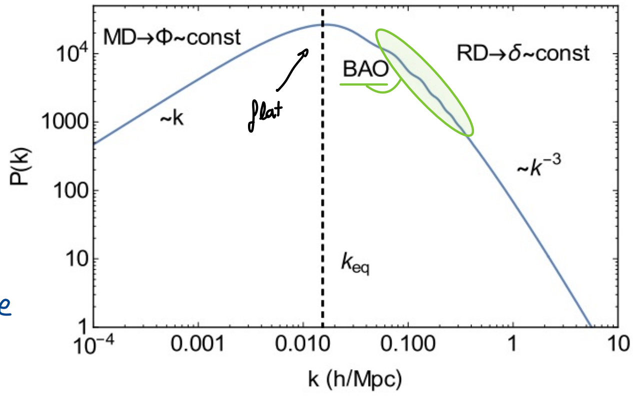

With these definitions, we can express $P(k)$ as:

$$P(k) = \langle \delta_k^2 \rangle = k^4 \langle \Phi_p^2 \rangle T(k)^2 \delta(a)^2 \sim k^4 k^{-3} k^{n_s-1} T(k)^2 \sim k^{n_s} T(k)^2$$

NOTE
$k_{eq} = 0.073 \Omega_{m,0} h$ (h/Mpc)
Scale that corresponds to the equallity between matter and radiation

And Using the Poisson equation:

$k \gg k_{eq} \longrightarrow \delta \sim \text{const} \rightarrow \Phi \sim \frac{1}{k^2} \rightarrow T \sim 1/k^2 \longrightarrow P(k) \sim k^{-3}$

$k \ll k_{eq} \longrightarrow \Phi \sim \text{const} \rightarrow \delta \sim k^2 \rightarrow T \sim 1 \longrightarrow P(k) \sim k$

Modes beyond k_{eq} (right hand side of the graph) enter the horizon during radiation domination. The transfer function behaves as:

$$T(k) = \begin{cases} 1/k^2 & k \gg k_{eq} \\ 1 & k \ll k_{eq} \end{cases}$$

And the power spectrum goes as:

$$\boxed{P(k) = \begin{cases} 1/k^3 & k \gg k_{eq} \\ k & k \ll k_{eq} \end{cases}}$$

Calculating the Fourier transform of $P(k)$, one obtains the two-point correlation function ($\xi(r)$) (~ prob. of galaxies at r)

$$\xi(r) = \frac{1}{2\pi^2} \int_0^\infty P(k)\, j_0(kr)\, k^2\, dk$$

$$\xi(r) = r^{-n-3} \qquad n = (1, -3)$$

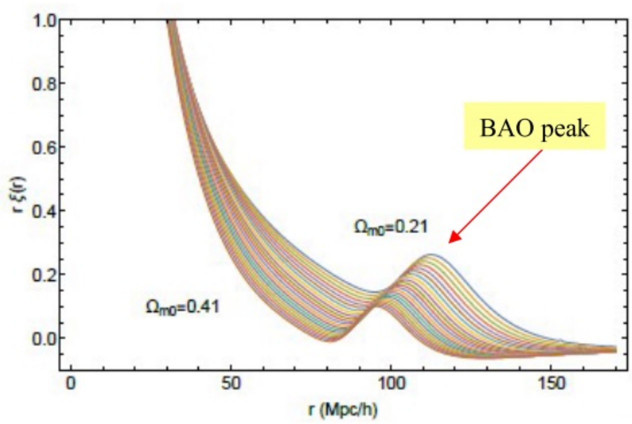

Discussion of Planck papers

The main Planck papers on the matter are 1807.06205, 1807.06209, 1807.06211

- Planck 2018 results. I. Overview, and the cosmological legacy of Planck
- Planck 2018 results VI. Cosmological parameters
- Planck 2018 results. X. Constrains on inflation

They discuss the main characteristics and frequencies:

Property	Frequency [GHz] 30	44	70	100	143	217	353	545	857
Frequency [GHz][a]	28.4	44.1	70.4	100	143	217	353	545	857
Effective beam FWHM [arcmin][b]	32.29	27.94	13.08	9.66	7.22	4.90	4.92	4.67	4.22
Temperature Sensitivity [μK_{CMB} deg][c]	2.5	2.7	3.5	1.29	0.55	0.78	2.56		
[kJy sr^{-1} deg][c]								0.78	0.72
Polarization Sensitivity [μK_{CMB} deg][c]	3.5	4.0	5.0	1.96	1.17	1.75	7.31		
Dipole-based calibration uncertainty [%][d]	0.17	0.12	0.20	0.008	0.021	0.028	0.024	~1	
Planet submm inter-calibration accuracy [%][e]	...	...	...	...	...	...	...	...	~3
Temperature transfer function uncertainty [%][f]	0.25	0.11	Ref.	Ref.	0.12	0.36	0.78	4.3	
Polarization calibration uncertainty [%][g]	< 0.01 %	< 0.01 %	< 0.01 %	1.0	1.0	1.0	...	...	...
Zodiacal emission monopole level [μK_{CMB}][h]	0	0	0	0.43	0.94	3.8	34.0	...	...
[MJy sr^{-1}][h]	...	...	...	...	...	...	...	0.04	0.12
LFI zero level uncertainty [μK_{CMB}][i]	±0.7	±0.7	±0.6	...	...	...	...	...	...
HFI Galactic emission zero level uncertainty [MJy sr^{-1}][j]	...	...	...	±0.0008	±0.0010	±0.0024	±0.0067	±0.0165	±0.0147
HFI CIB monopole assumption [MJy sr^{-1}][k]				0.0030	0.0079	0.033	0.13	0.35	0.64
HFI CIB zero level uncertainty [MJy sr^{-1}][l]	...	...	...	±0.0031	±0.0057	±0.016	±0.038	±0.066	±0.077

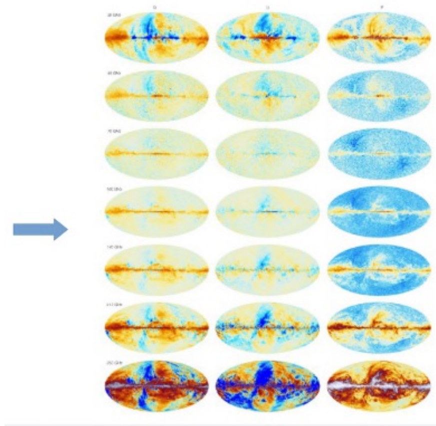

The position of the peaks

Extremum	Multipole	Amplitude [μK^2]
***TT* power spectrum**		
Peak 1	220.6 ± 0.6	5733 ± 39
Trough 1	416.3 ± 1.1	1713 ± 20
Peak 2	538.1 ± 1.3	2586 ± 23
Trough 2	675.5 ± 1.2	1799 ± 14
Peak 3	809.8 ± 1.0	2518 ± 17
Trough 3	1001.1 ± 1.8	1049 ± 9
Peak 4	1147.8 ± 2.3	1227 ± 9
Trough 4	1290.0 ± 1.8	747 ± 5
Peak 5	1446.8 ± 1.6	799 ± 5
Trough 5	1623.8 ± 2.1	399 ± 3
Peak 6	1779 ± 3	378 ± 3
Trough 6	1919 ± 4	249 ± 3
Peak 7	2075 ± 8	227 ± 6
Trough 7	2241 ± 24	120 ± 6

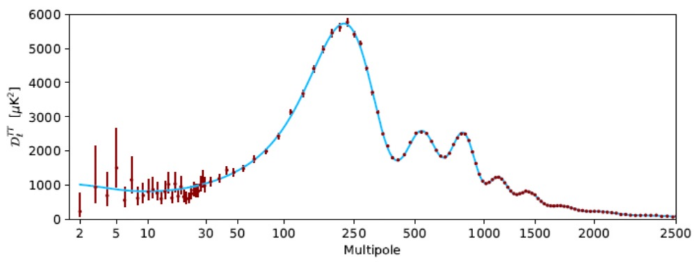

And the matter power spectrum in a six parameter ΛCDM model

Parameter	*Planck* alone	*Planck* + BAO
$\Omega_b h^2$	0.022383	0.022447
$\Omega_c h^2$	0.12011	0.11923
$100\theta_{MC}$	1.040909	1.041010
τ	0.0543	0.0568
$\ln(10^{10}A_s)$	3.0448	3.0480
n_s	0.96605	0.96824
H_0 [km $s^{-1}Mpc^{-1}$]	67.32	67.70
Ω_Λ	0.6842	0.6894
Ω_m	0.3158	0.3106
$\Omega_m h^2$	0.1431	0.1424
$\Omega_m h^3$	0.0964	0.0964
σ_8	0.8120	0.8110
$\sigma_8(\Omega_m/0.3)^{0.5}$	0.8331	0.8253
z_{re}	7.68	7.90
Age [Gyr]	13.7971	13.7839

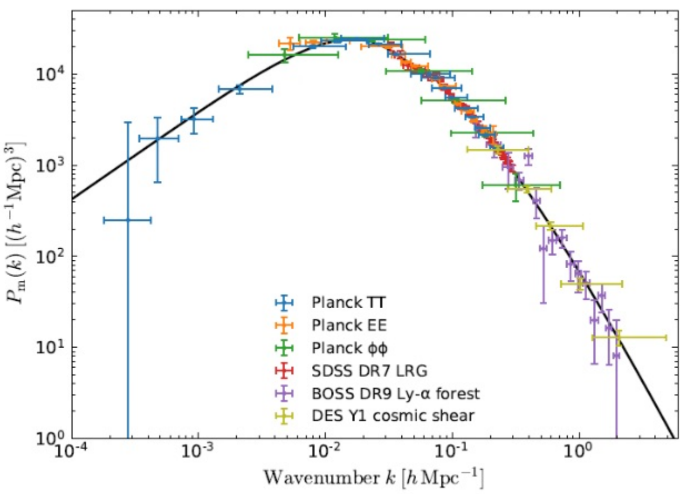

8.6. Boltzmann codes

Some existent codes

There are some codes to calculate the CMB anisotropies and power spectrum.

- CAMB: Code for Anisotropies in the Microwave background
  - + Code in f90, fast, recently updated, forum support
  - − code in f90, not very modular
- CLASS: Cosmic Linear Anisotropy Solving System
  - + Code in C++, recently updated, very modular (to introduce new models)
  - − Documentation a bit confusing sometime

CLASS

The variables and the equations

Once the cosmological parameters are introduced, the code solves the Friedmann equations:

$$\left(\frac{\dot{a}}{a}\right)^2 = \frac{8\pi}{3} G a^2 \bar{\rho} - K$$

$$\frac{d}{d\tau}\left(\frac{\dot{a}}{a}\right) = -\frac{4\pi}{3} G a^2 (\bar{\rho} + 3\bar{P})$$

And the perturbation equations for the metric (can choose between synchronous and conformal gauges):

i) Conformal Newtonian Gauge: $ds^2 = a^2(\tau)\{-(1+2\psi)d\tau^2 + (1-2\phi)dx^i dx_i\}$

ii) Synchronous gauge: $ds^2 = a^2(\tau)\{-d\tau^2 + (\delta_{ij} + h_{ij})\, dx^i dx^j\}$

The equations for each gauge are given by:

$$\begin{aligned}
k^2\phi + 3\frac{\dot{a}}{a}\left(\dot{\phi} + \frac{\dot{a}}{a}\psi\right) &= 4\pi G a^2 \delta T^0{}_0(\mathrm{Con}),\\
k^2\left(\dot{\phi} + \frac{\dot{a}}{a}\psi\right) &= 4\pi G a^2 (\bar{\rho} + \bar{P})\theta(\mathrm{Con}),\\
\ddot{\phi} + \frac{\dot{a}}{a}(\dot{\psi} + 2\dot{\phi}) + \left(2\frac{\ddot{a}}{a} - \frac{\dot{a}^2}{a^2}\right)\psi + \frac{k^2}{3}(\phi - \psi) &= \frac{4\pi}{3} G a^2 \delta T^i{}_i(\mathrm{Con}),\\
k^2(\phi - \psi) &= 12\pi G a^2 (\bar{\rho} + \bar{P})\sigma(\mathrm{Con}),
\end{aligned}$$

$$\begin{aligned}
k^2\eta - \frac{1}{2}\frac{\dot{a}}{a}\dot{h} &= 4\pi G a^2 \delta T^0{}_0(\mathrm{Syn}),\\
k^2\dot{\eta} &= 4\pi G a^2 (\bar{\rho} + \bar{P})\theta(\mathrm{Syn}),\\
\ddot{h} + 2\frac{\dot{a}}{a}\dot{h} - 2k^2\eta &= -8\pi G a^2 \delta T^i{}_i(\mathrm{Syn}),\\
\ddot{h} + 6\ddot{\eta} + 2\frac{\dot{a}}{a}\left(\dot{h} + 6\dot{\eta}\right) - 2k^2\eta &= -24\pi G a^2 (\bar{\rho} + \bar{P})\sigma(\mathrm{Syn}).
\end{aligned}$$

Basic code flowchart

1. User inputs main cosmological parameters Ω_m, Ω_b, n_s, H_0, ...
2. Calculate background evolution $H(z)$ and $a(t)$
3. The code solves perturbation equations of Botzmann hierarchy and multipoles $\Delta_\ell(k)$ for a grid of values of k, usually in $k \in [0.0001, 10]$ h/Mpc
4. Calculate matter power spectrum $P(k)$ and C_ℓ. Also, include other secondary effects.
5. Output results or feed MCMC code to estimate best-feed parameters.

After executing the code, the result is given in txt files with the C_ℓs.

$$T(\vec{x}, \hat{p}, \eta) = T(\eta)\left[1 + \Theta(\vec{x}, \hat{p}, \eta)\right]$$

$$\Theta(\vec{x}, \vec{p}, \hat{\eta}) = \sum_{\ell=1}^{\infty} \sum_{m=-\ell}^{\ell} a_{\ell m}(\vec{x}, \eta)\, Y_{\ell m}(\hat{p})$$

$$\langle a_{\ell m} \rangle = 0$$

$$\langle a_{\ell m}\, a^*_{\ell' m'} \rangle = \delta_{\ell\ell'}\, \delta_{mm'}\, C_\ell$$

It also returns the matter power spectrum, P_k, from the which we can obtain the two point correlation function (denotes probability of finding a galaxy at position r) as:

$$\xi = \frac{1}{(2\pi)^3} \int P(k)\, \frac{\sin(kr)}{kr}\, 4\pi k^2\, dk$$